ANEXO B

Artículos

"*Concatenation of a Fuzzy ARTMAP Neural Network to Different Variable Selection Techniques to Enhance E-Nose Performance*", Sensors and Actuators B (submitted).

Concatenation of a Fuzzy ARTMAP Neural Network to Different Variable Selection Techniques to Enhance An Electronic Nose Performance

C. Durán[1, 2], J.Brezmes[1], O.Gualdrón [1, 2], M.Vinaixa[1], E.Llobet[1], X.Vilanova[1], X.Correig[1]
[1]Departament d'Enginyeria Electrònica, Universitat Rovira i Virgili
Av. Paisos Catalans, 26. 43007 Tarragona (SPAIN)
e-mail: cduran@etse.urv.es, tel: (34) 977558764
[2]Departament of Electronic Engineering, University of Pamplona, Colombia

Abstract

This work compares the coupling of different variable selection techniques to a Fuzzy ARTMAP neural network in order to enhance an Electronic Nose performance. Based on a matrix of twelve metal oxide gas sensors (TGS and FIS), we designed an instrument to identify and classify different fungi species (from *Eurotium, Aspergillus*, and *penecillium* genres) that contaminate industrial bakery products. In this paper we present the classification results obtained for 7 fungal species using a Fuzzy Artmap paradigm coupled to different variable selection algorithms (DFA, PCA, Forward selection, intra-inter variance and Genetic Algorithms). Results show a boost in performance from a 43% with 12 variables (when no variable selection techniques are used) to a 75% using the combination of DFA and Fuzzy ARTMAP with just 2 variables.

Keywords: Variable Selection, Fungal Growth, Electronic Nose, Fuzzy Artmap, Genetic Algorithms, Forward selection, PCA, DFA

1. Introduction

Many microbial problems in bakery products are produced by fungal infections. The growth of these micro-organisms during storage are especially important in three different genres: *Eurotium*, *Aspergillus* and *Penicillium*. Microbial spoilage is a problem since it can induce nutritional losses, off-flavors and formation of mycotoxins or potentially allergenic spores [1]. Therefore, besides being an economic problem, unwanted fungal growth can cause some serious health hazards that have to be monitored carefully. Moreover, there is a growing pressure from governments and consumers to reduce the use of preservatives in intermediate moisture backery products, particularly those based on organic acids.

This is the reason why, nowadays, many researchers are looking for a method to conveniently assess the degree of fungal growth in bakery products at a very early stage and well in advance to becoming visible. The electronic nose (EN) promises to be one alternative for fungal detection in food products and that is why many studies have been reported on monitoring fungal contamination in bakery products [1-3] cereal grains [4-7], cheese [8], water [9], bread [10], meat [11] and milk [12].

However, although there are many commercial electronic noses available and many research studies have been performed on this particular subject, practical industrial applications have not yet been implemented, mainly due to Electronic nose high prices, difficult calibration, little reliability, poor reproducibility and low accuracy. In part, these problems are due to sensor noise and drift, which degrade the results that can be obtained.

For these reasons, it is very important to choose those variables (parameters and/or sensors) that contain the most useful and relevant information to the classification problem

envisaged. It is even more important to eliminate those variables with noisy or meaningless information that generate erroneous answers [13]. If the error sources could be identified and eliminated, more reliable and cheaper systems could be built since fewer sensors would be incorporated in the final configuration. However, serious studies on this subject have not been reported yet.

There are several variable selection techniques that can improve the performance of an Electronic Nose. The goal of this paper is to improve the response of an EN, enhancing the performance in the classification of seven fungal species. To do so, we have coupled different variable selection algorithms to a pattern recognition algorithm.

2. Theoretical background

A traditional way to reduce dimensionality is through Principal Component Analysis (PCA). PCA [14] is a method that uses principal components based on the variance of each original parameter. Each measurement is then projected against the new axis, the principal components. They can be used to extract the most relevant information from the entire data set. A sensor that has loading values near zero for the retained principal components contributes little to the overall model and can be eliminated. If two sensors have similar loadings they are highly collinear and one can be removed. However, PCA is a linear method that does not work very well in non-linear conditions.

Another classical method is Discriminant Function Analysis (DFA) [15], which is used to discriminate a set of measurements using the coefficients of the model's canonical variables. Like in PCA, the loadings (eigenvectors) are used to determine whether there are irrelevant or redundant sensors than can be removed. The main difference to PCA is that DFA is a supervised method that determines the variables to choose from the known classification of the training measurements of the application.

GAs (Genetic Algorithms) are optimization methods inspired on natural evolution. They have proven to be a remarkable good method for variable selection [16-19]. When this algorithm is applied for variable selection, a population of n subsets or chromosomes is created, each containing a random combination of variables. Chromosomes are binary strings where the occurrence of a bit equal to 1 (or 0) in position i-th implies that variable i-th is present (or absent). A cost function for each subset is then evaluated and, using techniques loosely based on biological genetics and evolution, a new population is then created. During the variable selection process, the cost function being optimized by the GA can be, for example, the prediction error of the fuzzy ARTMAP based classifier. In comparison to many other search techniques, GA's are not constrained by initial assumptions about the search space such as continuity and smoothness and, therefore, apply generally.

Another variable reduction method is through a ranking according to a figure of merit. The best option in this approach is to define a relationship between the average variance between measurements of the same category (internal variance, related to the repetitivity of the parameter) and the average distance between centroids of different categories (external

variance, related to the selectivity of the parameter). The criterion is defined to select an optimal subset of parameters, i.e., those showing a small internal variance combined with a high external variance [20]. This translates into selecting those variables with the highest discrimination power in the categorization problem under study. Equation 1 shows this criterion, which somehow measures the resolution power of each variable related to the differentiation between the categories to be identified

$$Vr = \frac{ExternalVariance}{InternalVariance} \quad (1)$$

Heuristic algorithms such as forward selection are widely used in linear regression [21-23]. Forward selection is quite simple and fast. Its main approach is to choose one variable at each iteration. Once the variable that gives the best prediction is selected, the process starts again trying to find the second variable that, combined with the first one, gives the best prediction ability to the system. The process ends when the prediction error increases adding any of the remaining variables.

All of the methods described above were coupled to a Fuzzy Artmap neural network [24-25]. This type of paradigm has been evaluated in electronic nose instruments for quite a few years now [26-27]. Theoretically, they have many advantages that make them very appealing to olfactory applications. Among their features, these networks require fewer samples to be trained (they learn very quickly), they are easy to program (they require less computational power than other paradigms), and they cope very well with drift situations (since they implement the stability-plasticity dilemma). Moreover, they do not need to be trained with a similar number of measurements of each category since they learn rare events very quickly.

Our main problem was the size of the data set, since for many learning paradigms, 16 is a low number of measurements, specially if 12 parameters are used. That's why this type of network was an ideal choice for the study.

3. Experimental

For the development of the Electronic Nose we used an array of 12 metal oxide sensors (SP series from FIS and 8-series from Figaro). A methacrylate chamber was designed to house these sensors. Table 1 describes each sensor used and its intended target vapours. Figures 1 and 2 show a couple of pictures of the Electronic Nose designed.

A HeadSpace AutoSampler (Hewlett Packard model 7694) was used to deliver the sample to the sensor chamber, so that a good reproducibility could be obtained. All sensor responses were acquired using a PCI-NI6023E data acquisition card. The control of the hardware, sampling equipment, data acquisition and signal processing was executed by a written-in-house program developed under the Matlab 6.5 environment. This software

allowed to monitor sensor output in real time and to obtain processed results very fast. The PARC algorithms used were PCA, DFA and the fuzzy ARTMAP neural network.

After ten days of incubation, a total of 19 vials (20 ml volume) were prepared. 14 contained 2 replicates of 7 fungal species and 2 contained empty cultivation mids. Finally, 3 vials of ethanol were used whether sensor drift was relevant. Table 2 describes the different samples used and the number of replicates. It also classifies each specie with its genre. The acquisition time for each sample was 10 minutes. For sample delivery, the following parameters in the sampling system were introduced: oven temperature between 70ºC-80ºC, 50 min vial heating time, 1 min vial pressurisation time, 1 min of loop fill time, 0.05 min of loop equilibration time, and 10 minutes of injection time. The carrier gas was regulated at a flow rate of 50 ml/min.

One parameter was extracted from each of the twelve sensors, namely the maximum conductance increment ($\Delta g_{max}=G_{max}-G_{min}$). Figure 3 shows a typical response from the sensor array to a fungal sample. Values plotted are resistive.

4. Results and discussion

As mentioned earlier, measured data were processed coupling Fuzzy ARTMAP neural networks to different variable selection algorithms. In all cases, a leave-one-out approach was used to estimate the performance of the network in the classification of fungi species.

This iterative validation approach generates N evaluation procedures (1 for each measurement). At each iteration, a different measurement is left out, while the remaining ones are used to build the model (PCA, DFA, etc) and train the network. The measurement not used for training is then projected onto the model and classified using the already trained network. This is repeated N times (one for each measurement) so that the final result is the average outcome of the entire iterative process (see figure 4).

This approach is very convenient in cases were the experimental data set does not contain many measurements (like in our case). Another important point of this methodology is that the performance of the approach is what is evaluated, rather than a particular trained network since, in fact, N networks are created and evaluated using the same procedure. Moreover, since the measurement left out for evaluation is not used for training, there is no risk on getting unrealistic results due to over-fitting.

4.1. Fuzzy ARTMAP classifier

First, in order to compare the results, a fuzzy ARTMAP neural network was used alone to identify the samples from 7 fungi species using all the sensors (12 variables). The classification success rate into eight categories reached a 43 % using the leave-one-out approach (if the identification was made at random, a 12.5% should be expected).

Once this classification rate was obtained, the goal was to couple different variable selection techniques to the fuzzy ARTMAP paradigm to see whether this approach improved results.

4.2. Using DFA as a variable selection technique

DFA can be used in supervised and in unsupervised mode. In unsupervised mode it can give interesting information about the clustering of the dataset. Anyway, for serious benchmarking, a supervised mode has to be used where the training measurements should be different from the test data set, which is the way we have performed our leave-one-out approach.

At each iteration, a DFA model was built with the training measurements. Then, the coordinates of the training samples in the DFA projection were used to train a Fuzzy ARTMAP neural network. The evaluation measurement was projected onto the DFA model and its coordinates fed to the neural network. Eigenvectors were used to classify samples. A 75% success rate was achieved using only 2 eigenvectors. These results were expected due to the clusters of fungal genres and species that the DFA graphics show in figures 5 and 6. It is important to remember that when using a leave-one-out cross-validation method, the over-fitting risk is eliminated since the evaluation measurement has not been used to build the DFA model.

4.3. PCA used as a variable selection method coupled to fuzzy ARTMAP

In the PCA projection on figure 7 it can be seen that using a mean centring pre-processing most of the variance (more than 85%) relies on the first PC. Moreover it can be deduced that a 2 PC model captures more than 99% of the information, an indication that the number of variables with meaningful information can be greatly reduced.. In the figure it can be seen that there is overlapping between eurotium and penicillium genres and the cultivation mids.

At each iteration, a PCA model was calculated with the training measurements and the scores were fed to a fuzzy ARTMAP for training purposes; then, with the PCs calculated and the weights from the Fuzzy ARTMAP, the validation measurement was projected and evaluated. Results with different number of principal components were tested. The best results were achieved with just 2 PC's, where a classification rate of 63 % was achieved.

4.4. Results coupling Genetic Algorithms and fuzzy ARTMAP:

A genetic algorithm coupled to the fuzzy ARTMAP classifier selected 5 out of 12 variables. The fitness was evaluated as the PER (Predictor Error Rate) and the cross-validation of order one (leave-one-out) with 16 measurements was applied. The PER was 0.3556 and the algorithm converged after 33 generations. The success rate was 63 %.

4.5. Variable selection using the intra/inter variance criterion

As mentioned in the previous section, a variance criterion was defined in order to reduce the number of variables.. A higher value for Vr meant a better discrimination capability for a given variable. Figure 8 shows the Vr values for each of the 12 sensors/variables.

Fuzzy ARTMAP was applied to evaluate the variable subset selected. The best results where obtained when selecting the 7 variables (circled in the graphic) with the highest *Vr*.The success rate peaked at 63 %.

4.6. Forward selection

The forward selection algorithm used in linear regression was applied in our case to select a subset of the 12 original variables. In the end, only 2 variables were selected. Using these variables, the success rate achieved was 70 %.

Table 3 summarises the results obtained, comparing the coupling of different variable selection techniques to a fuzzy ARTMAP classifier. We can observe that applying any of the variable selection methods leads to better results than using the Fuzzy ARTMAP alone.

As it can be seen, the best results are achieved coupling Fuzzy Artmap algorithms with DFA, with a 75% success rate when classifying samples in 8 categories (seven fungi species and a control vial without fungal contamination). Moreover, it is interesting to note the performance of the forward selection method (70%), since it gives very good results and the variables selected are sensors from the original array, giving a straightforward interpretation (sensor selection) that can be used to reduce the dimensionality of the array for a given application. That is why this method should be studied in greater detail for each application sought for an electronic nose.

5. Conclusions

Although the number of measurements is not enough to generalize the results obtained, the work performed in this experimental data set strongly suggests that coupling variable selection techniques (e.g., GA, DFA, PCA and heuristic algorithms) to a Fuzzy ARTMAP neuronal network can improve significantly the performance of an Electronic Nose classifier system for fungi identification. Best results were obtained coupling DFA to a Fuzzy ARTMAP neural network using only 2 variables (factors) instead of 12. More interesting is the result obtained with Forward Selection, whose results directly translate into a selection of the sensors that should be used in a real application.

Although a more complete study should be performed to generalize these results, it is quite clear that the manufacture of electronic noses equipped with variables selection algorithms could increase the industrial interest of these instruments in food applications since their reliability and accuracy would increase and their price would drop due to a reduction on the sensor array dimensions.

Acknowledgements

This work was funded by FIS (Thematic Network C03/08).

References

[1] Magan, N, Volatiles as an Indicator of fungal activity and differentiation between species and the potential use of electronic nose technology between for early detection of grain spoilage, Journal Stored Products Research, 36, (2000), pp. 319-340.

[2] Needham, R. Magan, N.; Detection and differentiation of microbial spoilage organisms of bakery products in vitro and in situ. 2002,9th ISOEN, Technical Digest, pp. 240-241.

[3] Needham, R,"Early detection and differentiation of spoilage of bakery products", Sensors and Actuators B, vol 106, (2005), pp: 1.

[4] Magan, N.; Evans, P.;Volatiles as an indicator of fungal activity and differentiation between species, and the potential use of electronic nose technology for early detection of grain spoilage. Journal of Stored Products Research, 2000, 36, 319-340.

[5] Olsson, J; Börjesson, T; Lundstedt, T; Schnürer, J.; Volatiles for mycological quality grading of barley grains: determinations using gas chromatography–mass spectrometry and electronic nose. International Journal of Food Microbiology,2000,59, 167–178.

[6] Olsson, J; Börjesson, T; Lundstedt, T; Schnürer, J.; Detection and quantification of ochratoxin A and deoxynivalenol in barley grains by G-MS and electronic nose. International Journal of Food Microbiology, 2002, 72, 203-214.

[7] Börjesson, T, Eklöv. T, Jonsson. A, Sundgren. H, Schnürer, J. Electronic Nose for Odor Classification of Grains, Cereal Chem, 1996, 73(4): 457-461.

[8] Trihaas, J, Tatjana van den Tempel, Per Vaeggemose Nielsen, Electronic nose: Smelling the microbiological quality of cheese, Proceddings on ISOEN, Rome, 2002, pp 380-384.

[9] Shin, H. W.; Llobet, E; Gardner, E; Hines, E.L; Dow, C.S; Classification of the strain and growth phase of cyanobacteria in potable water using an electronic nose system. IEEE Proc-Sci. Meas. Technol., 2000, 147(4), 158-164.

[10] Keshri, G; Voysey, P; Magan, N. Early detection of spoilage moulds in bread using volatile production patterns and quantitative enzyme assays. Journal of Applied Microbiology, 2002, 92(1), 165-172.

[11] Vernat-Rossi, V; Garcia, C; Talon, R; Denoyer, C; Berdagué, J.L; Rapid discrimination of meat products and bacterial strains using semiconductor gas sensors. Sensors and Actuators B, 1996, 37, 43-48.

[12] Magan. N; Pavlou. A; Chrysanthakis, I; Milk-sense: a volatile sensing system recognise spoilage bacteria and yeast in milk. Sensors and Actuators B, 2001, 72, 28-34.

[13] Pearce, T.C. et al, "Handbook of machine olfaction", electronic nose technology, Wiley, (2003), pp. 325-345.

[14] Cadima, J,"Computational aspects of algorithms for variables selection in the context of principal components", Computational Statics & Data Analysis, 47 (2004), pp: 225-236.

[15] Klecka, William R. (1980). Discriminant Analysis. Quantitative Applications in the Social Sciences Series, No. 19. Thousand Oaks, CA: Sage Publications.

[16] Llobet E., J. Brezmes, O. Gualdrón, X. Vilanova, X. Correig, Building parsimonious fuzzy ARTMAP models by variable selection with a cascaded genetic algorithm: application to multisensor systems for gas analysis*, Sensors and Actuators B*, 99 (2004) 267-272

[17] Gardner J.W., P. Boilot, E.L. Hines, Enhancing electronic nose performance by sensor selection using a new integer-based genetic algorithm approach*, Sensors and Actuators B*, 106 (2005) 114-121.

[18] Broadhurst D., R. Goodacre, A. Jones, Genetic algorithms as a method for variable selection in multiple linear regression and partial least squares regression, with applications to pyrolysis mass spectrometry, Anal. Chim. Acta, 348 (1997) 71-86.

[19] Gardner J., P. Bartlett, Electronic Noses: Principles and Applications, Oxford Science Publications, Oxford, 1999

[20] Brezmes, J., "Discrimination between different samples of olive oil using variable selection techniques and modified fuzzy ARTMAP neuronal networks", 9th ISOEN, Rome, (2002).

[21] Miller, A.J, "Subset selection in regression" Chapman & Hall, London, (1990).

[22] Paulsson N., E. Larson, F. Winquist, Extraction and selection of parameters for evaluation of breath alcohol measurement with an electronic nose, Sensors and Actuators A, 84 (2000) 187-197.

[23] Lu Xu, Wen-Jun Zhang, Comparison of different methods for variable selection, Anal. Chim. Acta, 446 (2001) 477-483.

[24] Carpenter G.A., S. Grossberg, D.B. Rosen, Fuzzy ART: Fast stable learning and categorization of analog patterns by an adaptive resonance system, Neural Networks, 4 (1991) 759

[25] Carpenter G. A., S. Grossberg, N. Markuzon, J. H. Reynolds, and D. B. Rosen, "Fuzzy ARTMAP: A neural network architecture for incremental supervised learning of analog multidimensional maps," IEEE Trans. Neural Networks, vol. 3, pp. 698--713, Sept. 1992.

[26] Llobet, E.; Hines, E.L.; Gardner, J.W.; Franco, S., Non-destructive banana ripeness determination using a neural network based electronic nose, Measurement Science & Technology (1999), vol. 10, pp.538-548

[28] Brezmes, J.; Llobet, E.; ; Vilanova, X.;.Saiz, G.; Correig, X.; Orts, Correlation between electronic nose signals and fruit quality indicators onshelf-life measurements with pinklady apples Sensors and Actuators B (80), 2001, pp. 41-50

Figure captions

Figure 1. Exterior picture of the Electronic Nose designed

Figure 2: Inner parts of the Electronic Nose

Figure 3: Gas sensor response (resistance) as a function of time under the analysis of the headspace of a fungi vial.

Figure 4: Block diagram of the cross-validation approach

Figure 5: DFA clustering of fungal species

Figure 6: DFA clustering of fungal genres

Figure 7: Discrimination of Fungi species with a PCA

Figure 8: Vr values for each sensor. Circled crosses are the selected variables

Figure 1

Figure 2

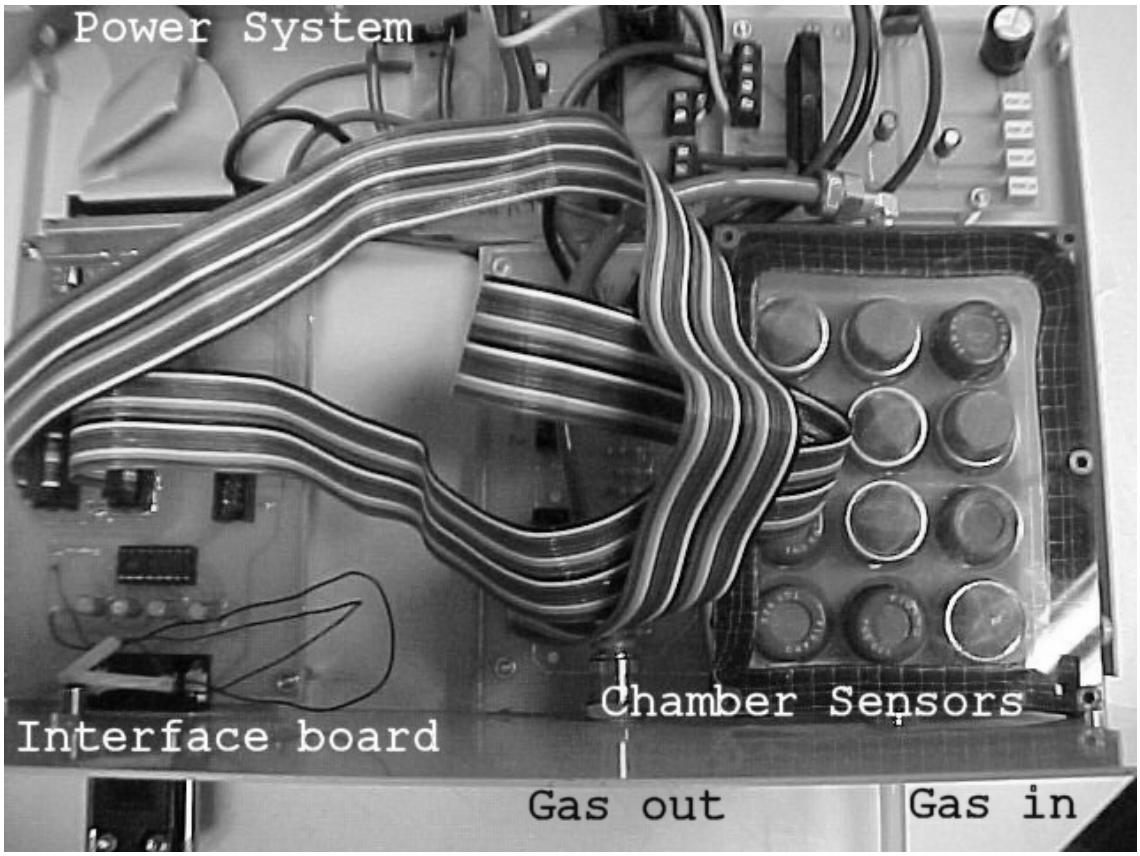
Power System
Chamber Sensors
Interface board
Gas out
Gas in

Figure 3

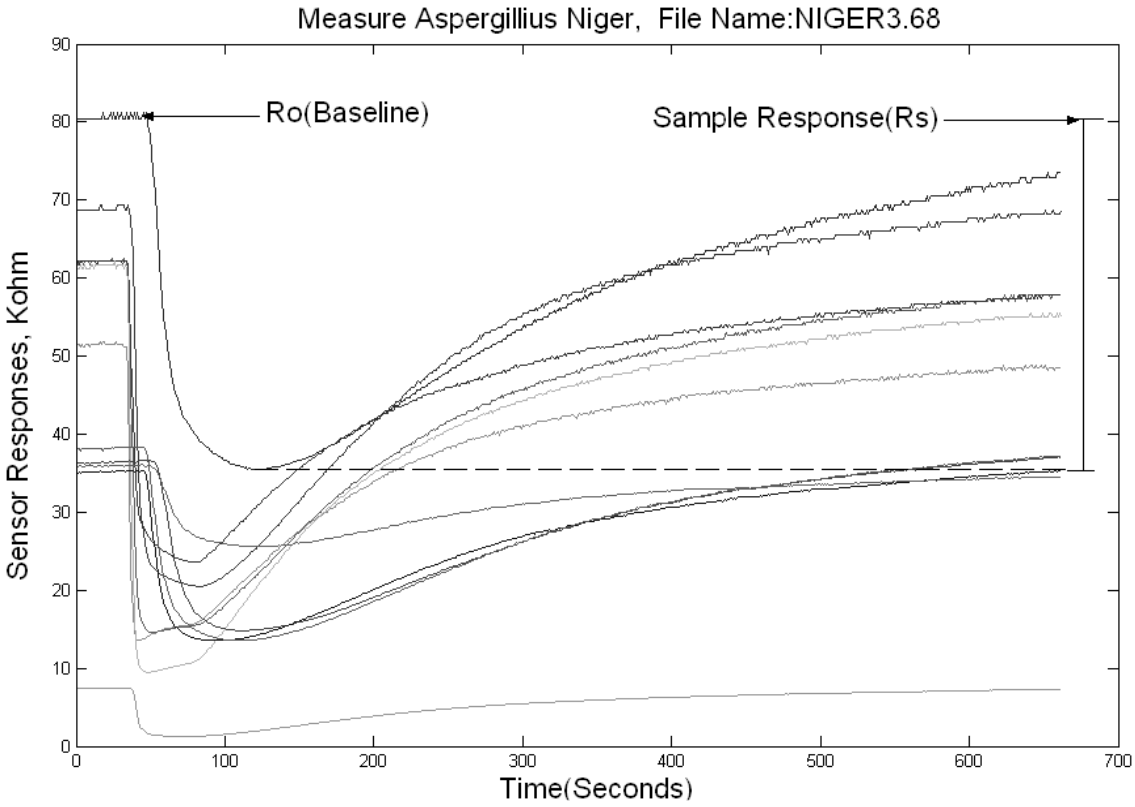
Measure Aspergillius Niger, File Name:NIGER3.68
Ro(Baseline)
Sample Response(Rs)
Sensor Responses, Kohm
Time(Seconds)
0
10
20
30
40
50
60
70
80
90
0
100
200
300
400
500
600
700

Figure 4

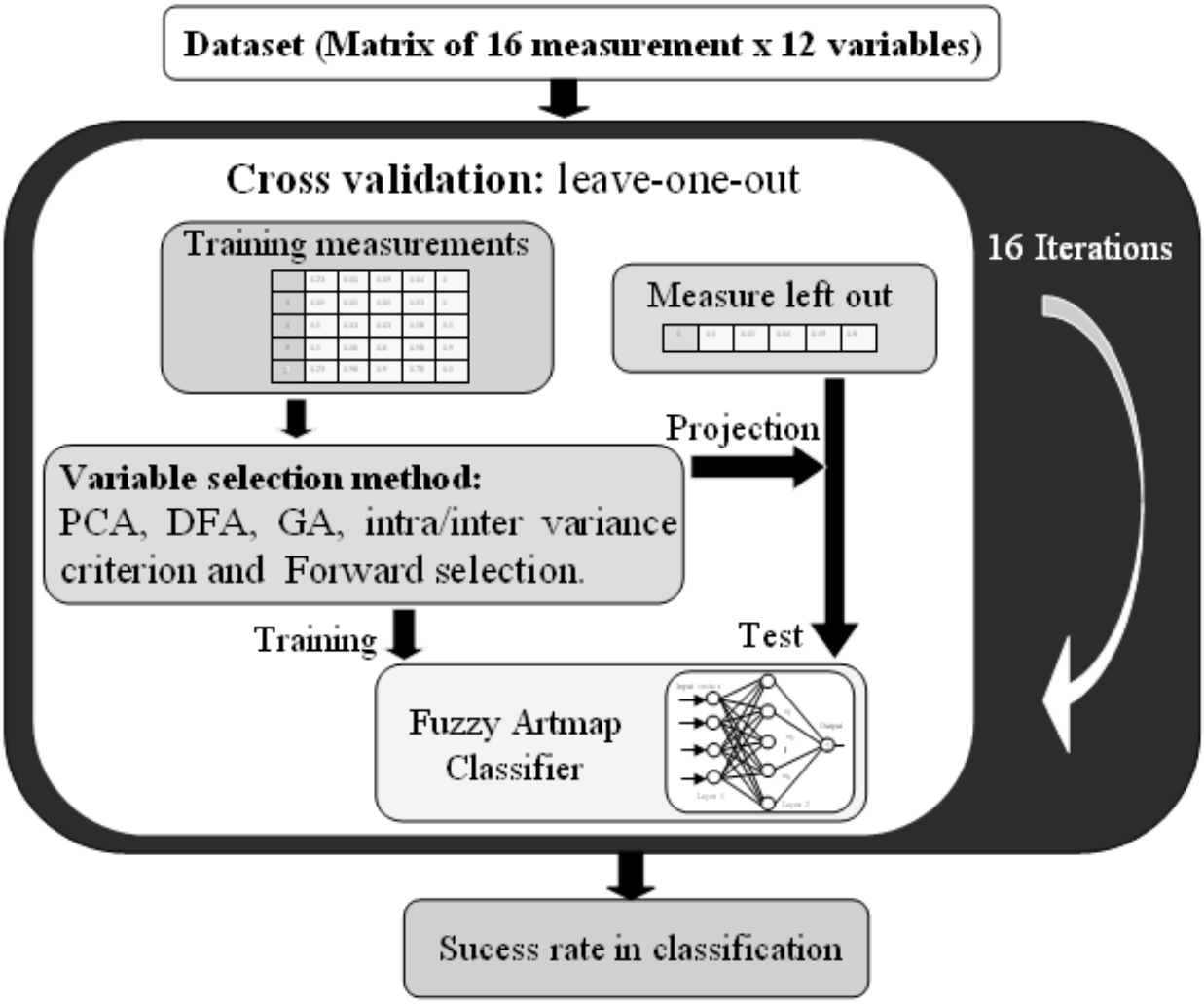
Dataset (Matrix of 16 measurement x 12 variables)
Cross validation: leave-one-out
16 Iterations
Training measurements
Measure left out
Projection
Variable selection method:
PCA, DFA, GA, intra/inter variance criterion and Forward selection.
Training
Test
Fuzzy Artmap Classifier
Sucess rate in classification

Figure 5

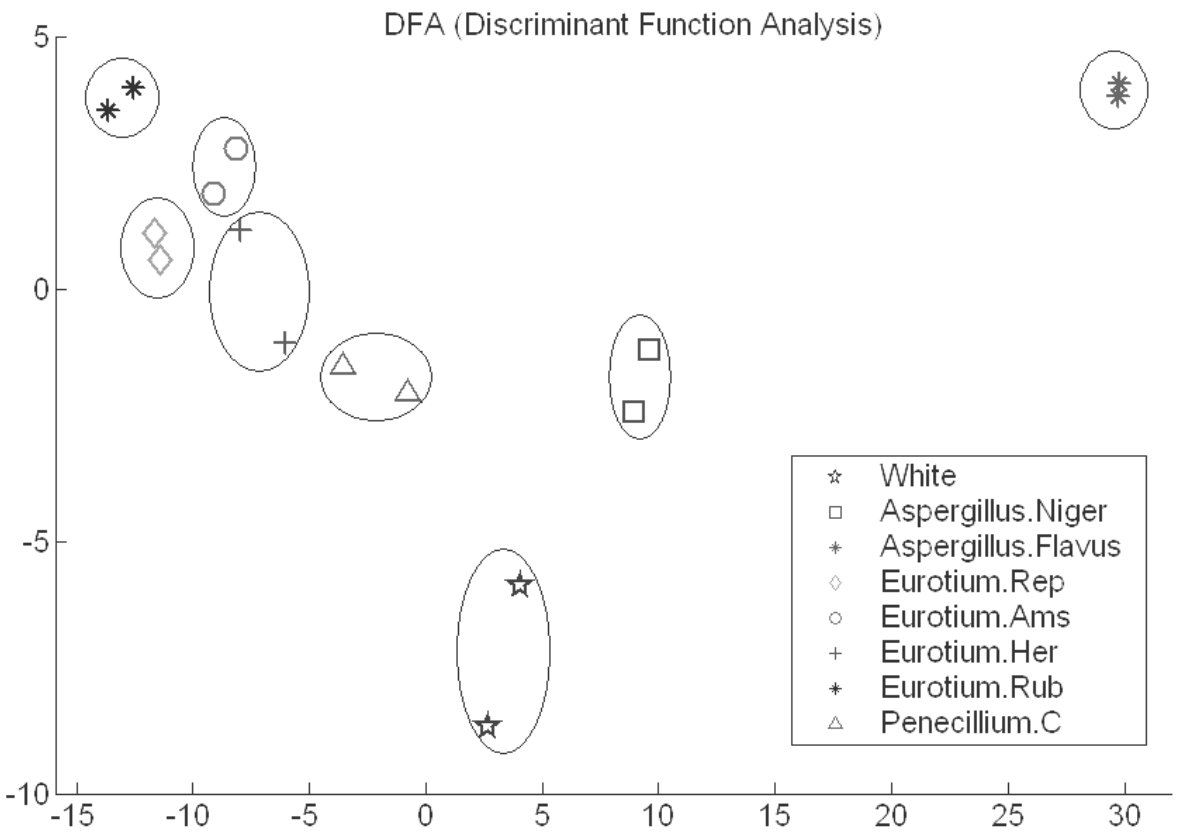
DFA (Discriminant Function Analysis)
5
0
-5
-10
-15
-10
-5
0
5
10
15
20
25
30
White
Aspergillus.Niger
Aspergillus.Flavus
Eurotium.Rep
Eurotium.Ams
Eurotium.Her
Eurotium.Rub
Penecillium.C

Figure 6

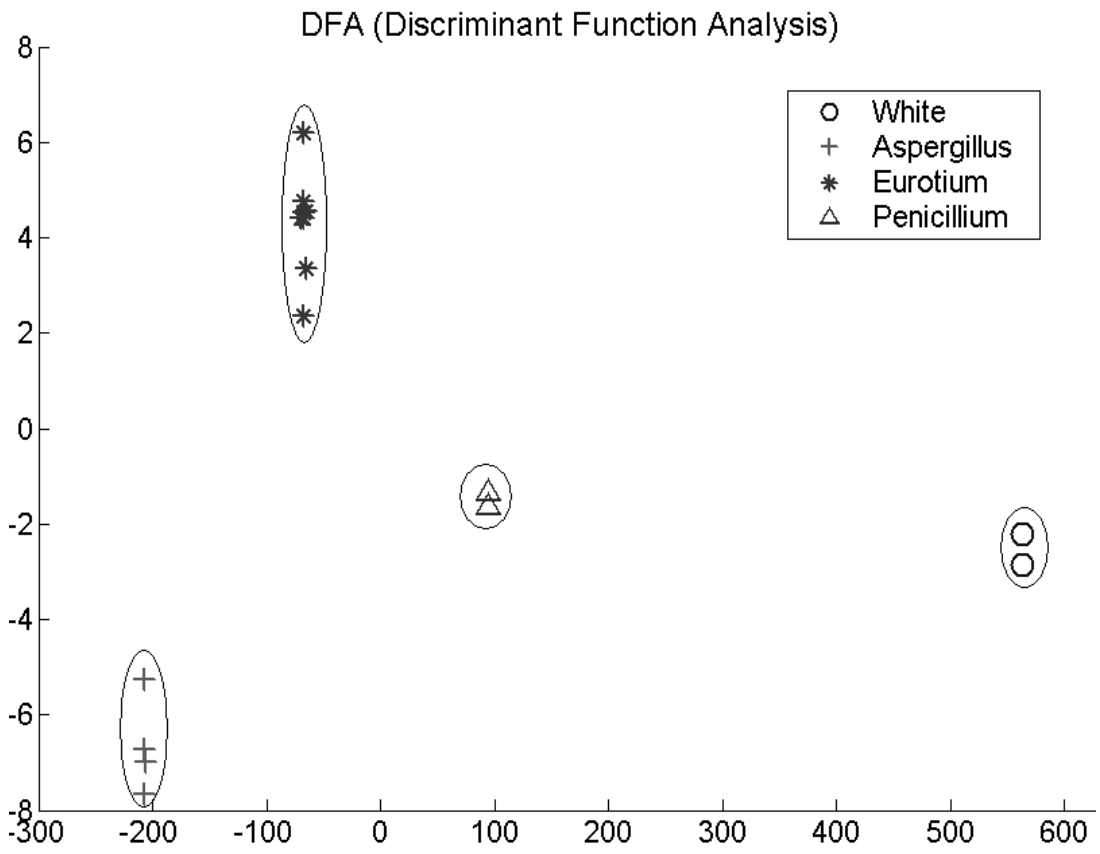
DFA (Discriminant Function Analysis)
White
Aspergillus
Eurotium
Penicillium
8
6
4
2
0
-2
-4
-6
-8
-300
-200
-100
0
100
200
300
400
500
600

Figure 7

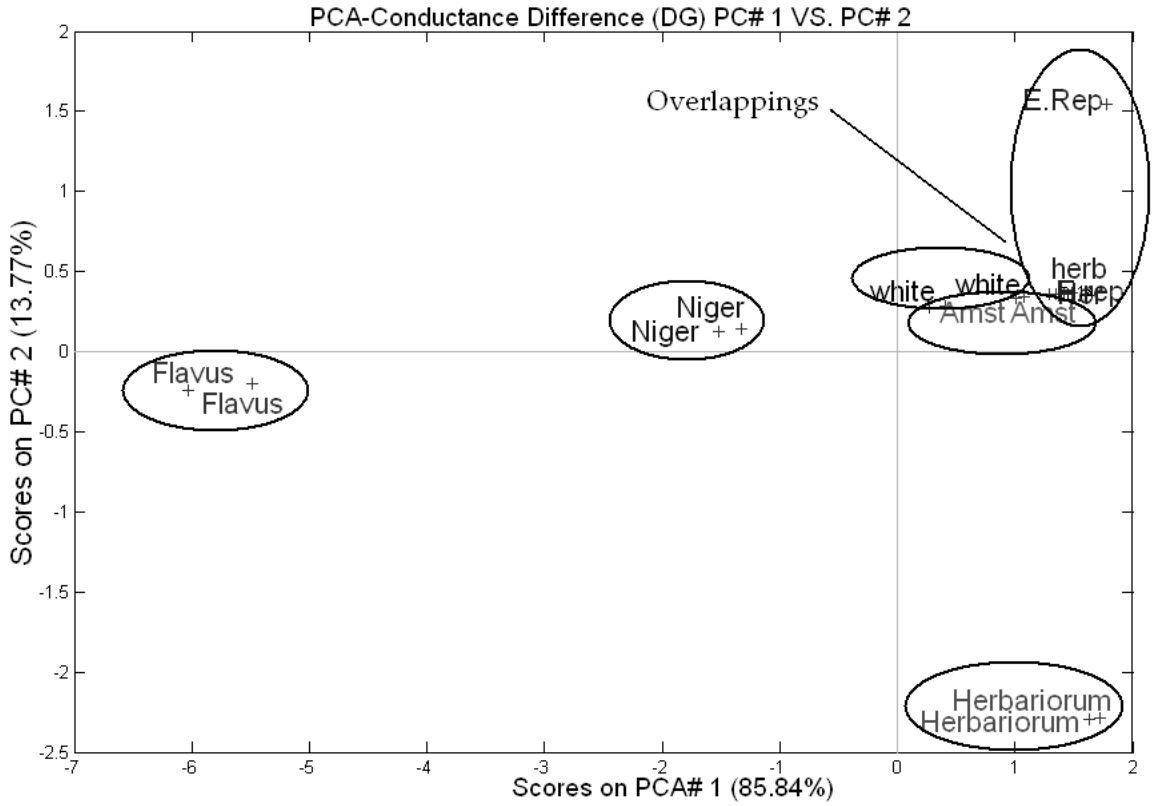
PCA-Conductance Difference (DG) PC# 1 VS. PC# 2
Overlappings
E.Rep
herb
white
white
Amst
Amst
Niger
Niger
Flavus
Flavus
Herbariorum
Herbariorum
Scores on PC# 2 (13.77%)
Scores on PCA# 1 (85.84%)
2
1.5
1
0.5
0
-0.5
-1
-1.5
-2
-2.5
-7
-6
-5
-4
-3
-2
-1
0
1
2

Figure 8

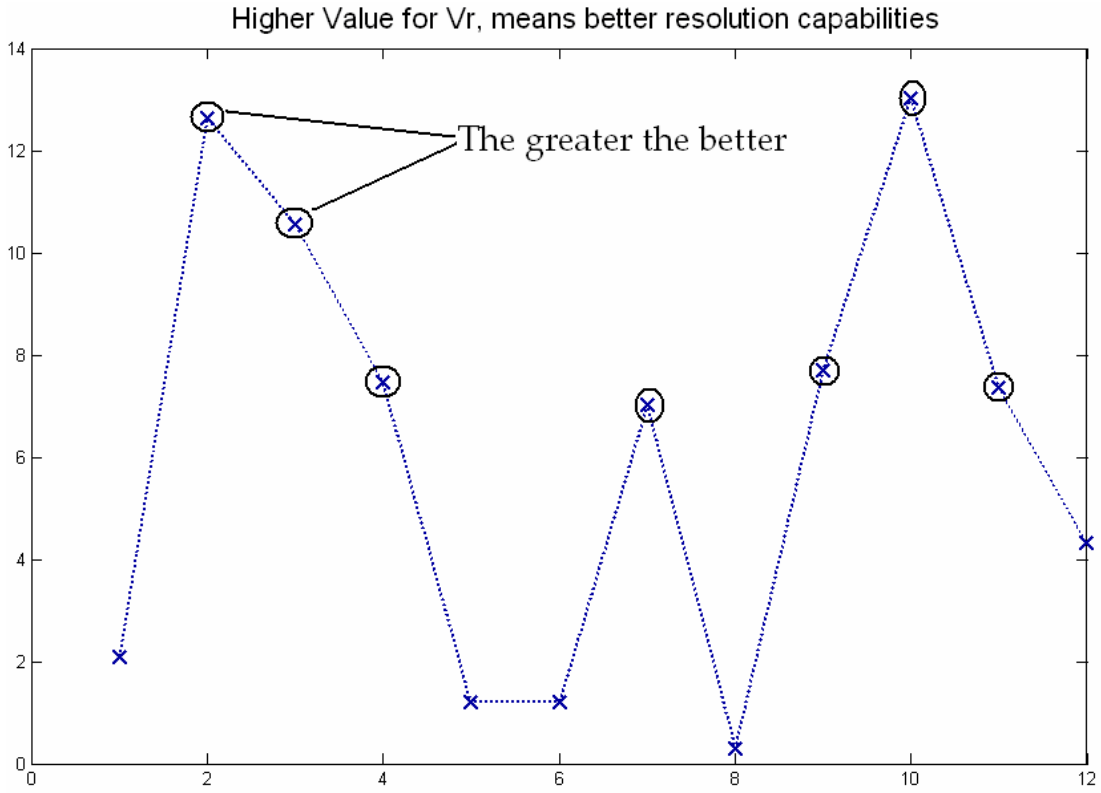
Higher Value for Vr, means better resolution capabilities
The greater the better
0
2
4
6
8
10
12
14

Table captions

Table 1. Sensors array description

Table 2. Fungal Species measured

Table 3. Variables selected.

Table 1. Sensors array description

Sensor	**Target vapours**
TGS 800	Air contaminants
TGS 813	Combustible gas
TGS 822	Alcohol, toluene, *o*-xylene, etc
TGS 825	Hydrogen sulphide
TGS 826	Ammonia
TGS 831	R-21-R-22
TGS 832	R-134a, R-22
TGS 842	Methane, butane, propane
TGS 880	Volatile species from food
TGS 882	Alcohol vapours from food
FIS SP-31-00	Organic solvents
FIS SP-32-00	Alcohol

Table 2. Fungal Species measured

Genre/specie	Replicates
Eurotium Repens	2
Eurotium Herbariorum	2
Eurotium Amstelodami	2
Eurotium Rubrum	2
Aspergillus flavus	2
Aspergillus Niger	2
Penicillium Corylophilum	2

Table 3. Variables selected.

Methods	**Results**	**Subset selected**
Fuzzy ARTMAP alone	43%	12
DFA+ Fuzzy ARTMAP	75%	7
PCA+ Fuzzy ARTMAP	63%	7
GA+ Fuzzy ARTMAP	63%	5
Vr criteria	63%	7
Forward + Fuzzy ARTMAP	70%	2

"Enhancing sensor selectivity through flow modulation", Sensors and Actuators B, (submitted), (2005).

Enhancing sensor selectivity through flow modulation

C.Duran
Department of electronic engineering
University of Pamplona
Pamplona, Colombia
cristhian.duran@urv.net

J.Brezmes,E.Llobet,X.Vilanova, X.Correig
Departament d'enginyeria electrònica, elèctrica i Automatica
Universitat Rovira i Virgili
Tarragona, Spain
jesus.Brezmes@urv.net

Abstract—In this paper, a new method to enhance sensor selectivity is described. A flow modulation system driven by a PC-controlled peristaltic pump has been designed to feed a sensor chamber with different vapors. 45 measurements where performed comprising five different species (benzene, toluene, o-xylene, methanol and para-xylene) in three different concentrations (20, 200, 2000 ppm). Using frequency domain techniques and neural networks, the system was able to reach a 92% classification success rate when identifying all five vapors despite concentration was not constant and a single sensor was used. Moreover, when amplitude and variance information were removed from sensor transient signals, a 62% success rate was achieved, proving that the transient waveform has additional information that helps to enhance selectivity.

Introduction

In the last ten years, considerable efforts have been made to use sensor dynamics as a source of multivariate information leading to an enhancement in the discriminating ability of poorly-selective metal oxide gas sensor arrays.

Hand-held 'sniffers' make use of simple sample delivery units based on pumps rather than mass-flow controllers. Because it is well known that sensor dynamics can be of help to increase the selectivity of metal oxide sensors, there is a need for developing uncomplicated methods to use transient information in such analyzers.

In fact, many authors have reported on strategies based on modulating either the sensor operating temperature [1] or the analyte concentration [2,3]. Here we introduce and demonstrate, for the first time, a simple method that combining simultaneously both effects has the potential of increasing the resolving power of metal oxide sensors. Furthermore, its simplicity makes it especially suited for low-cost applications.

The new method presented here consists of applying a modulated control signal to the peristaltic pump of a sniffer, which results in the gas flow being modulated. The effect of this flow modulation is twofold: First, the concentration of analytes at the surface of sensors is modulated and second, fast periodical flow changes result in periodical cooling and heating of sensors' surface. Therefore, specific response patterns, which are characteristic of the analytes present, develop. The method can be easily adapted to both static and dynamic headspace sampling strategies. Here we show that it is possible to easily discriminate among five different vapors (benzene, toluene, methanol, o-xylene and para-xylene) in a broad concentration range using a single sensor.

Section 2 describes the experimental set-up, while section 3 describes the measurements performed and discusses the results obtained. Finally, section 4 outlines the conclusions and describes future work in this direction.

EXPERIMENTAL SET-UP

To achieve a flow-modulation capable electronic nose, we designed a closed loop system, based on a PC controlled peristaltic pump. Figure 1 shows the configuration devised.

The system has two operating modes. In the cleaning configuration, synthetic dry air enters the system through the first electro-valve and cleans the peristaltic pump, the sensor chamber and the evaporation chamber. Solid arrows mark the flow of clean air in this mode.

In measuring mode, air re-circulates around a closed circuit. Once the modulation is initiated, a chromatographic syringe sprays a calculated quantity of liquid contaminants into the evaporation chamber. Clean air inside the circuit becomes contaminated when forced to re-circulate around the evaporation chamber thanks to the peristaltic pump. Dashed arrows show this circuit.

A microcontroller commands the speed of the peristaltic pump which directly translates into different flow rates. A PC programmed with a written-in-house user friendly program communicates with the microcontroller so that the user can select the frequency and flow rate waveform that has to be applied. Through this program, the PC commands the microcontroller to open or close the electro-valves to change the configuration of the system depending upon the operating mode desired.

Moreover, the PC records the sensor response (in terms of conductivity). Figure 2 shows the transient signals developed by the modulated sensors. It is important to remark that only a small section of the entire transient is used for the analysis. Specifically, the part used is from the time interval when the sensor modulated signals show a stable and periodic behaviour. Then, signal pre- and post-processing algorithms are applied to identify the vapor sample measured.

Liquid quantities of the contaminants measured were calculated and sprayed into the contaminants chamber using a chromatographic syringe. A total of 45 measurements were

performed. The measurements comprised five different vapors (benzene, toluene, methanol, o-xylene and para-xylene) at three different concentrations (20,200,2000 ppm) with three replicates for each type of measurement.

Then, a periodic pulse modulation with a frequency of 10 mHz and an amplitude of 250 sscms was applied. Figure 3 shows a typical response from a sensor to five different contaminants when flow is pulsed as described above.

Three different sensors were used for the measurements. Table 1 lists their designation and main applications. Their information was never combined to obtain better results, since the main goal of the experiment was to determine how selective each single sensor could get by itself using the flow modulation approach.

An FFT was applied to the periodic response and its amplitude value was considered (see figure 4). Values for the fundamental and harmonic frequencies were used as output data from the sensors and fed to a Fuzzy Artmap pattern recognition algorithm.

RESULTS AND DISCUSSION

All results obtained and listed in Table 2 were performed using a cross-validation of order 1 (the so-called leave-one-out approach). The goal was to classify measurements in five different categories, one for each contaminant , with the added difficulty of variable concentration (20, 200 and 2000 ppm).

Different preprocessing strategies were used to determine how much the mean amplitude, variance and waveform from each sensor response contributed to the classification of the 45 measurements.

Figure 5 shows, for sensor TGS 823, the different transient modulated signals for each measurement. Different colors (or gray scales) refer to the species measured, comprising all three concentrations.

From the figures it can be derived that some of the classification success rate achieved without preprocessing of the transient signals (see figure 5a) is due to mean value (i.e. static

parameters). Moreover, when mean value is removed (figure 5b) some information from the variance could be used for the classification of the five species. Finally, in figure 5c all mean and variance information is removed and if there is some kind of classification it will be due to waveform rather to any kind of amplitude information.

From the results exposed in table 2 it is clear that best results are obtained when the evolution of sensor conductance through time is not preprocessed.

Anyhow, considering that classifying samples into 5 categories at random would yield a 20% success rate, it is clear that sensor response without mean value or even unbiased and scaled by its variance still retain useful information since classification rates never fail below a 53%.

CONCLUSIONS

A new modulation method has been tested to increase sensor selectivity. A wide range of concentrations and contaminants have been tested confirming that flow modulation allows for a reliable identification of different vapor species.

Additional work has to be done to optimize the system and test the approach under tougher conditions like binary or tertiary vapor mixtures.

Acknowledgment **(Heading 5)**

This work has been funded by FIS thematic network C03/08

References

[1] Llobet, E.; Brezmes, J.; Ionescu, R.; Vilanova, X.; Al-Khalifa, S.; Gardner, J.W.; Bârsan, N.; Correig, X. "Wavelet Transform and Fuzzy ARTMAP Based Pattern Recognition for Fast Gas Identification Using a Micro-Hotplate Gas Sensor", Vol: 83, pp. 238-244, 2002.

[2] E. Llobet, X. Vilanova, J. Brezmes, J.E. Sueiras and X. Correig, "Transient response of thick-film tin oxide gas sensors to multicomponent gas mixtures" Sensors and Actuators B, Vol: 47, pp. 104-112, 1998.

[3] E.Llobet, X.Vilanova, J.Brezmes, R. Alcubilla, J. Calderer, J. Suerias and X. Correig, “Conductance-transient analysis of thick-film tin oxide gas sensors under successive gas-injection steps”, Meas. Science and Technology, Vol: 8, pp. 1133-1138, 1997.

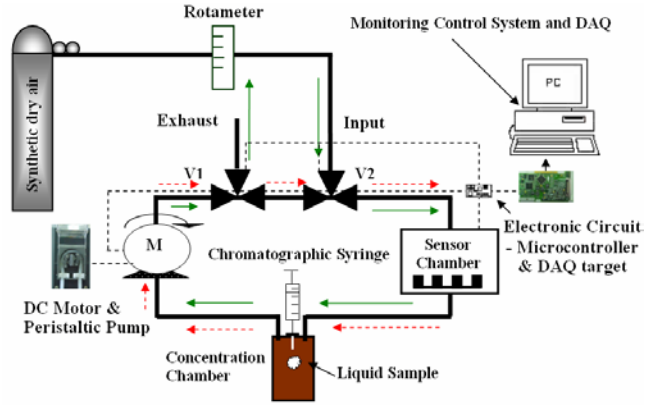

Figure 1: Schematic diagram of the flow modulation system

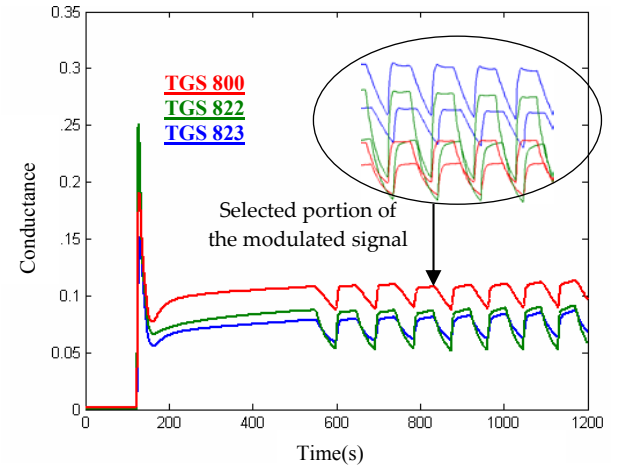

Figure 2: Sensor transient signals with (right) and without (left) flow modulation

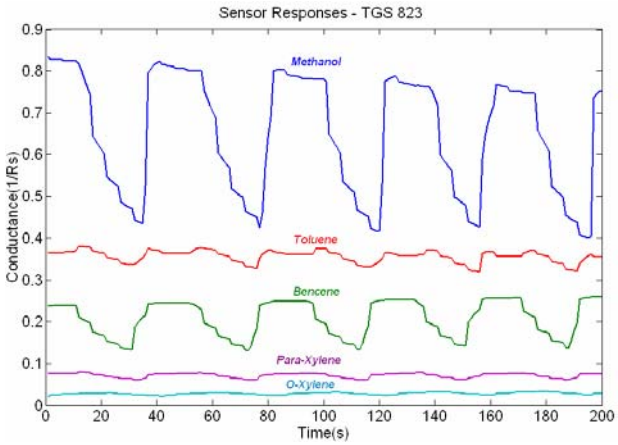

Figure 3: Typical responses to five different contaminants

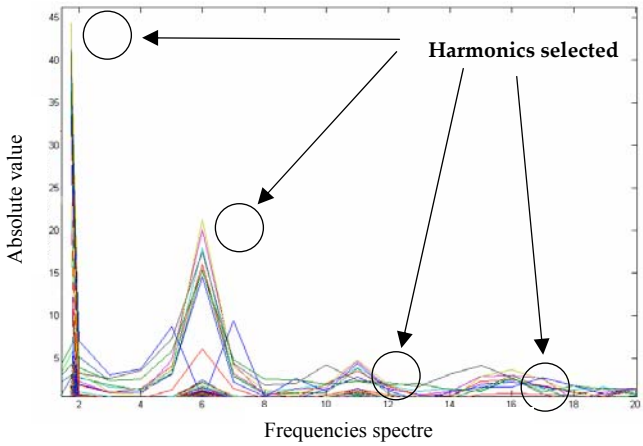

Figure 4: Harmonics selected from the FFT response of the transient signals from one sensor for different species and concentrations

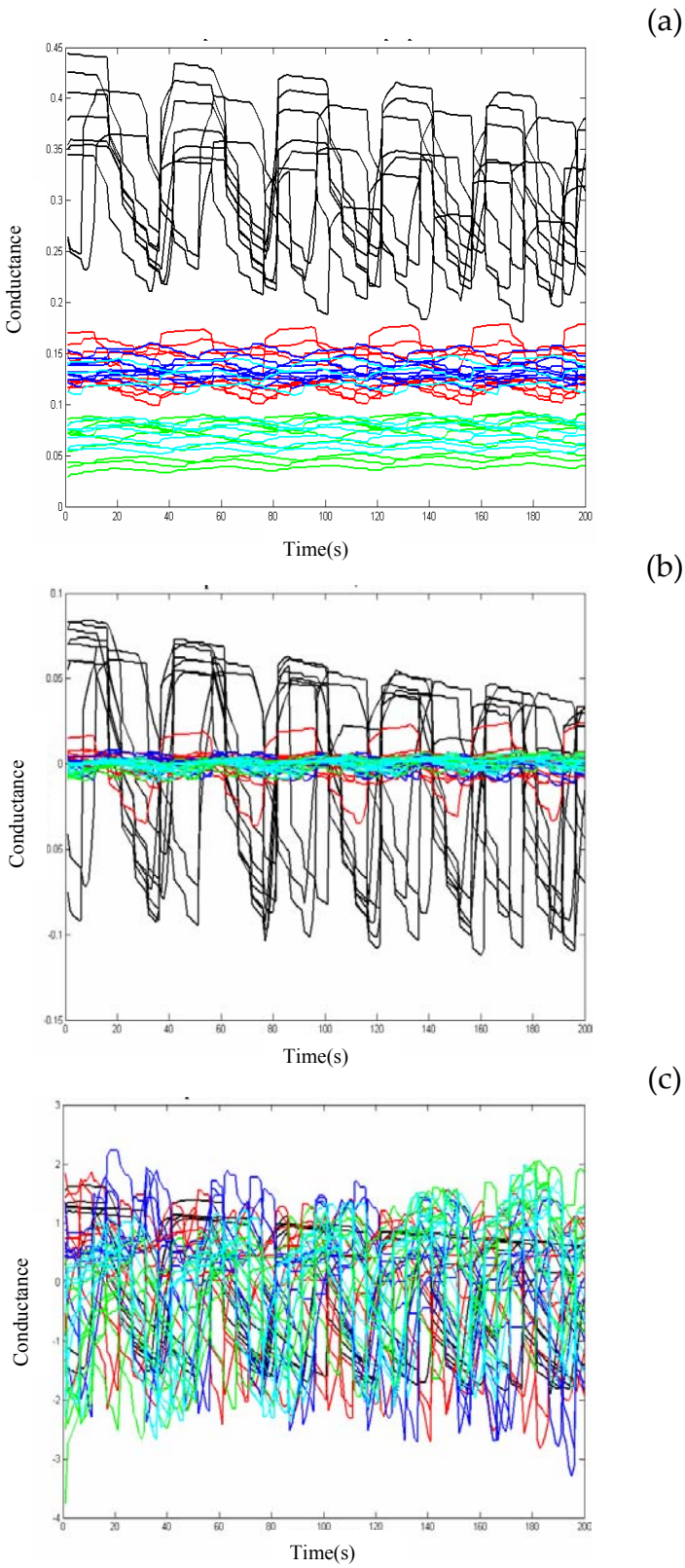

Figure 5: Transient modulated responses from sensor 800. (a) non-processed; (b) mean-centered; (c) auto-scaled

Sensor	Main application
TGS 800	Air Quality control
TGS 822	Alcohol detection
TGS 823	Organic Dissolvent

Table 1: Sensors used and their main applications

Pre-processing	TGS 800	TGS 822	TGS 823
None	Learning rate: 0.7 Harmonics: 10 Succes rate: 84%	Learning rate: 1 Harmonics: 17 Succes rate: 93%	Learning rate: 1 Harmonics 4 Succes rate: 91%
Mean centering	Learning rate: 0.9 Harmonics: 13 Succes rate: 82%	Learning rate: 0.8 Harmonics: 17 Succes rate: 82%	Learning rate: 0 Harmonics 7 Succes rate: 80%
Auto-scaling	Learning rate: 0.1 Harmonics: 4 Succes rate: 53%	Learning rate: 0.7 Harmonics: 5 Succes rate: 62%	Learning rate: 0 Harmonics 15 Succes rate: 55%

Table 2: Classification rate for normalization strategy

"Detection of 20 ppb's of benzene on a CO_2 flow using semiconductor gas sensors and a thermal desorption system", Sensors and Actuators B, (submitted), (2005)

"Detection of 20 ppb's of benzene on a CO2 flow using semiconductor gas sensors and a thermal desorption system"

C.Durán[1,2], J.Brezmes[1], E.LLobet[1], X.Vilanova[1], J.M. Sánchez[3], X.Correig[1]

[1]Departament d'Enginyeria Electrònica, Universitat Rovira i Virgili
Av. Paisos Catalans, 26. 43007 Tarragona (SPAIN)
e-mail: cduran@etse.urv.es, tel: (34) 977558764
[2]Departament of Electronic Engineering, University of Pamplona, Colombia
[3]University of Gerona, (SPAIN)

Abstract: A new multisensor system including a thermal desorption unit has been designed to detect benzene traces in a CO_2 flow. The system uses a carbopack unit that absorbs benzene traces and then releases them concentrated in a factor greater than 200. is capable of classifying benzene samples down to 10 ppb's in a CO_2 flow with different volatile interferences. This is the first time that such a system has been designed.

1. INTRODUCTION

The safety and quality control of food products is becoming a priority issue in developed countries. This means that new and more restrictive legislation is being issued by governments to answer the public awareness of the situation. In the case of gaseous beverages such as sodas and beers, the quality of the CO_2 used is of vital importance to comply with the recommendations of the ISBT (International Society of Beverage Technologists), [**1**].

To cope with newer legislation requirements, expensive instruments are being used to control CO_2 quality at the production plant [**2, 3**]. Nevertheless, these instruments do not provide on-line analysis and they require specialized personnel to operate them. Moreover, they cannot be used in the transportation of the stage or in the customer plant, phases where the product can be contaminated by external sources.

The work presented in this paper has been developed to address a real need by a CO_2 production plant in Spain. The main goal of the application that will be described is devoted to the detection of benzene down to the values recommended by the ISBT (around 5-10 ppb's) in a CO_2 flow with a 99.95% purity level. Even at this purity value, many interfering volatiles can still be found, as described in table 1. These requirements should be achieved with a cheap and reliable system that could be easily installed, operated and maintained at the customer facilities or even embedded in the transportation system.

To achieve such ambitious goals a carefully devised research and development effort has been planned. The first stage of such a plan is to design a prototype to evaluate the feasibility of the approach selected.

For the first time, a prototype based on a semiconductor multisensor array coupled to a thermal desorption unit has been proposed to detect benzene under a CO_2 flow.

The coupling of thermal desorption units to multisensor systems based on semiconductor gas sensors to enhance their sensibility has been proposed before [**4-7**]. Anyhow, these systems have never been used under a CO_2 atmosphere, since the general belief that tin oxide gas sensors need oxygen to interact have prevented their use in this type of applications. Nevertheless, recent publications prove that these type of sensors perform in a similar way under a CO_2 atmosphere. Moreover, in the prototype designed a novel and simple made-in-house design has been proposed and tested for the thermal desorption unit.

This paper has been organized in four different sections. The second chapter describes the prototype fabricated, including the design process followed until the definitive prototype has been completed. Section 3 describes the results obtained and discusses the suitability of the instrument designed to the application sought. Finally, section four outlines the conclusions of our work.

2. SYSTEM DESIGN

2.1 General configuration

The system initially proposed consists of four different electro-valves, a platform with the thermal desorption unit, a sensor chamber, electronic circuitry and a Personal Computer system to control de measurement process, acquire sensor signals and to process those signals into useful information. Figure 1 shows the configuration proposed.
The measurement process starts when electro-valves 1 and 4 redirect the CO_2 flow to the adsorption system as the dashed line illustrates. In this configuration, benzene impurities are absorbed in the carbon powder during a predefined period of time. Once the concentration phase is finished, the thermal desorption phase can be activated using the same circuit or in the other direction, changing the position of electro-valves 2 and 3. Electro-valve 5 has been included to maintain the same flow in the sensor chamber no matter the measurement phase.

The sensor chamber houses a minimum amount of sensors (4) in order to minimize the dead volume of the system and the energy consumption. A software controls the measurement process in real-time so that the system completes each measurement in the same way in order to obtain a repetitive set of measurements.

2.2 Sensor array design and optimisation

Two different sensor chambers were designed for the system. The first chamber (seen in figure 2) was specifically designed to determine which sensors were going to be housed in the final prototype. With that goal on mind, the chamber was capable of housing up to 15 sensors at the same time.

Using the first chamber, measurements were performed to determine the sensitivities of 21 different sensors against benzene. Table 2 describes the sensors tested. In order to be sure about which sensors were more sensitive to benzene, concentrations of 20, 7, 5 and 2 ppm's were measured with all 22 sensors. Table 3 describes the sensors chosen after determining the best sensitivities (defined as the normalized conductance increment).

The final chamber housed the four most sensitive sensors against benzene. Figure 3 shows how the chamber was fabricated. The dead volume was minimized to 0.6 ml with external dimensions of 10x10x6 mm.

2.3 Design and fabrication of the thermal desorption unit

The thermal desorption unit envisaged for the system had to comply with three different features:

- High temperature heating, up to 350ºC, since carbon concentrators need a temperature higher than 300ºC to be activated and to be cleaned completely.
- Low thermal inertia to be able to ramp up temperature as fast and accurate as possible
- Easy coupling of temperature proves to accurately monitor heating temperature

Different systems were proposed and carefully evaluated. Figure 4 shows a schematic diagram of the approach chosen in the end. Table 4 shows the temperatures and transient times achieved by this system. Figure 5 shows a real picture of the device constructed. The tube was filled with Carbopack B absorbent. Table 5 shows the characteristics of this material. Temperature was controlled using a k-type thermocouple. Figure 6 shows the electronic circuit connected to the thermocouple used.

2.4 System automation

In order to obtain repetitive results, the whole measurement process had to be automated. In fact, the automation of the equipment was one of the initial premises that had to be proved if the system ever becomes commercially available. A PC was in charge of the measuring process, controlling the following devices:

- All the electro-valves
- A current controlled source, with a maximum amperage of 4 amps.
- The sensor chamber

Figure 7 shows the final system configuration with the different subsystems. Different lines show the different pathways that could be used. One possibility is to use the solid line for both absortion and desorption. A second possibility is to use the dashed line for absorption and the solid line for desorption.

3. RESULTS AND DISCUSSION

3.1 Experimental design

Figure 8 shows the chronogram of the measurements made with the prototype. Initially, synthetic dry air cleans the adsorbent during 20 minutes, to make sure there are no rests from previous measurements. After that, contaminated CO_2 (with a given concentration of benzene) was directed through in the adsorption tube during 10 minutes. After those ten minutes, a flow of CO_2 was applied during two minutes to stabilize the sensor response before applying the current to heat the adsorbent, which lasted ten additional minutes. After that, 8 additional minutes where used to cool the system.

With this approach, 200ºC where reached during the desorption phase and 25ºC after the cooling period. In most of the cases a second desorption cycle was performed in order to assure the complete desorption of the benzene. Figure 9 shows the sensor array response to three consecutive desorptions. It can be seen that after the first desorption cycle, the second and third bear no sensor response, assuring that the first one desorbed completely the benzene concentrated.

3.2 Measurements

Measurements were performed with adsorption of 150, 70, 20 and 10 ppb's of benzene under a CO_2 flow. Tables 6, 7 and 8 shows the different mixtures measured with 10 ppb's and 20 ppb´s of benzene and their codification, where it can be seen that clean CO_2 and CO_2 plus other interferences were also included in the measurement set to classification.

3.3 Results

Figure 10 shows a PCA graph were it can be seen the different clusters corresponding to different types of measurements. It is clear that the system devised is able to discriminate measurements with as low as 10 ppb's compared to pure CO_2 or CO_2 with other interfering species.

A fuzzy artmap neural network was applied with a leave-one-out approach to see how well a neural network could distinguish between the different situations. Tables 9 and 10 show the results considering a classification comprising all the species, a categorization between 20 ppb, 10 ppb and no benzene samples and presence/absence of benzene.

From the results it is clear that the system is capable of detection reliably up to 10 ppb's of benzene despite the presence of other interfering species.

4. CONCLUSIONS

We have demonstrated how a multisensor system based on semiconductor gas sensors is able to detect down to 10 ppb's of benzene under a CO2 atmosphere despite the presence of other contaminant species. The use of a cheap made-in-house thermal desorption unit has the potential to boost sensitivity between 100 to 500 times the one showed by the sensor system alone, making the detection of ppb traces of benzene possible in such application.

References

[1] ISBT carbon dioxide quality guidelines and analytical procedure bibliography, internacional Society of Beverage Technologists, USA, March 2001.

[2] R.L Firor, B. D. Quimby, Analysis of trace sulfur compounds in beverage grade carbon dioxide, Agilent Technologies Inc., USA April 2, 2001.

[3] Trace Impurities in Beverage-Grade CO_2 Incorporating the Amperometric Sulfur Detector. PerkinElmer, Inc, USA, http://www.perkinelmer.com/. (2005).

[4] Leonello Dori, Sergio. N, Ivan. E, Anna. R. Mastrogiacomo, Laura. S, Elisabetta. P, "*A Gas Chromatographic-like System for the Separation and Monitoring of Benzene Toluene and Xylene Compounds at the ppb Level Using Solid State Metal Oxide Gas Sensors"*, Istituto di Scienze Chimiche "F. Bruner", University of Urbino, Italy, (2000).

[5] T. Rechenbach, J. Nieß, P. Boeker, U. Schramm, G. Horner, S. Rösler, G. Krauskopf, S. Winter, E. Weber, J. Bargon, P. Schulze Lammers, *Improvement of the Sensitivity of an Ammonia Gas Sensor Based on a Quartz Microbalance by Thermal Desorption,* The 13th European Conference on solid-State Transducers (Eurosensors XIII), September 12-15 , The Hague, The Netherlands, pág:705-708, (1999).

[6] F.Bender, N. Barié, G. Romoudis, A. Voigt, M. Rapp, *Development of a preconcentration unit for a SAW sensor micro array and its use for indoor air quality monitoring*, Sensors and Actuators B, Vol : 93, Pág : 135-141, (2003).

[7] Tim. H, J. Niess, P. Schulze L, B. Diekmann, P. Boeker, *" Online measurement of odorous gases close to the odour threshold with a QMB sensor system with an integrated preconcentration unit"* Sensors and Actuators B, Vol: 95, pág: 39-45, (2003).

Figures

Tables

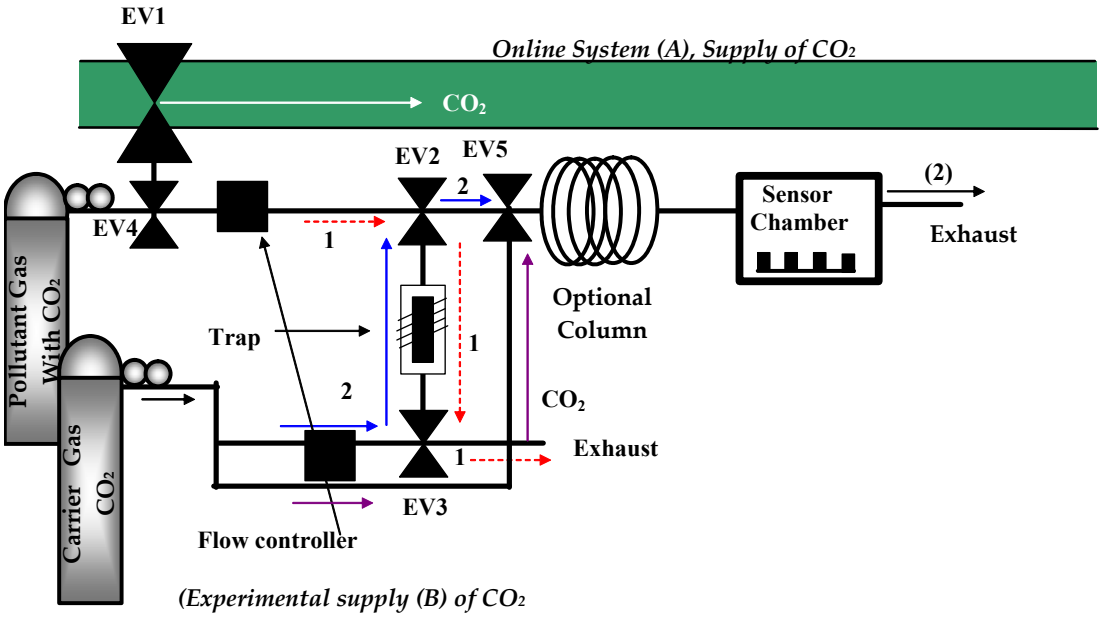

Figure 1: Plant of the prototype

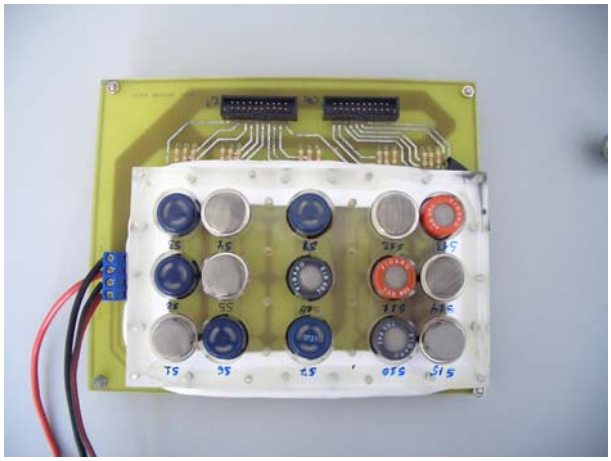

Figure 2: Sensor chamber, capacity 15 commercial sensors (FIS and taguchi TGS)

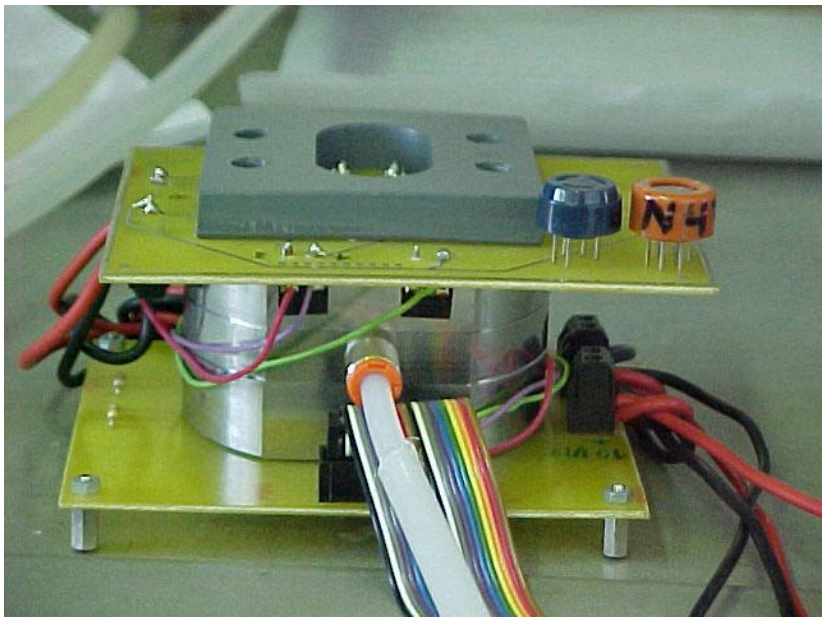

Figure 3: Sensor chamber fabricated with dead volume

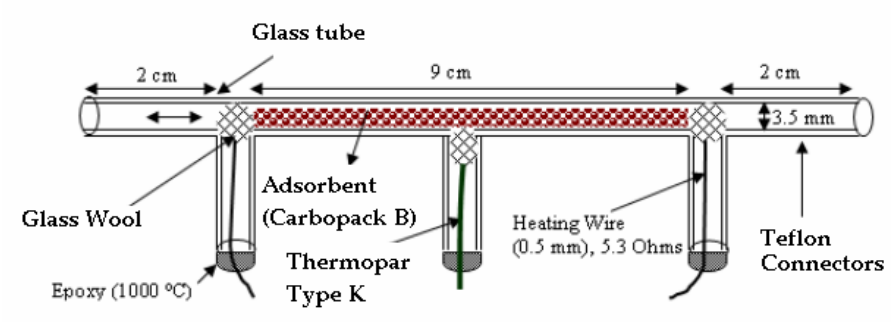

Figure 4: Schematic diagram of the approach chosen in the end.

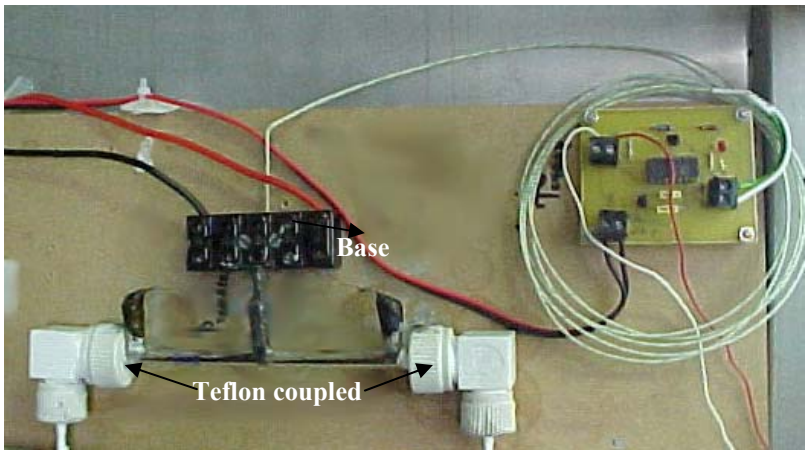

Figura 5: Termal desortion unit constructed

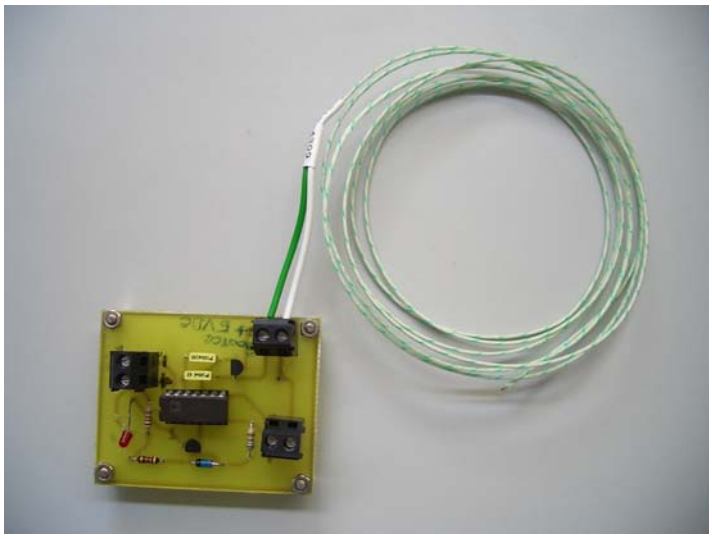

Figura 6: Control circuit (Thermopar type k)

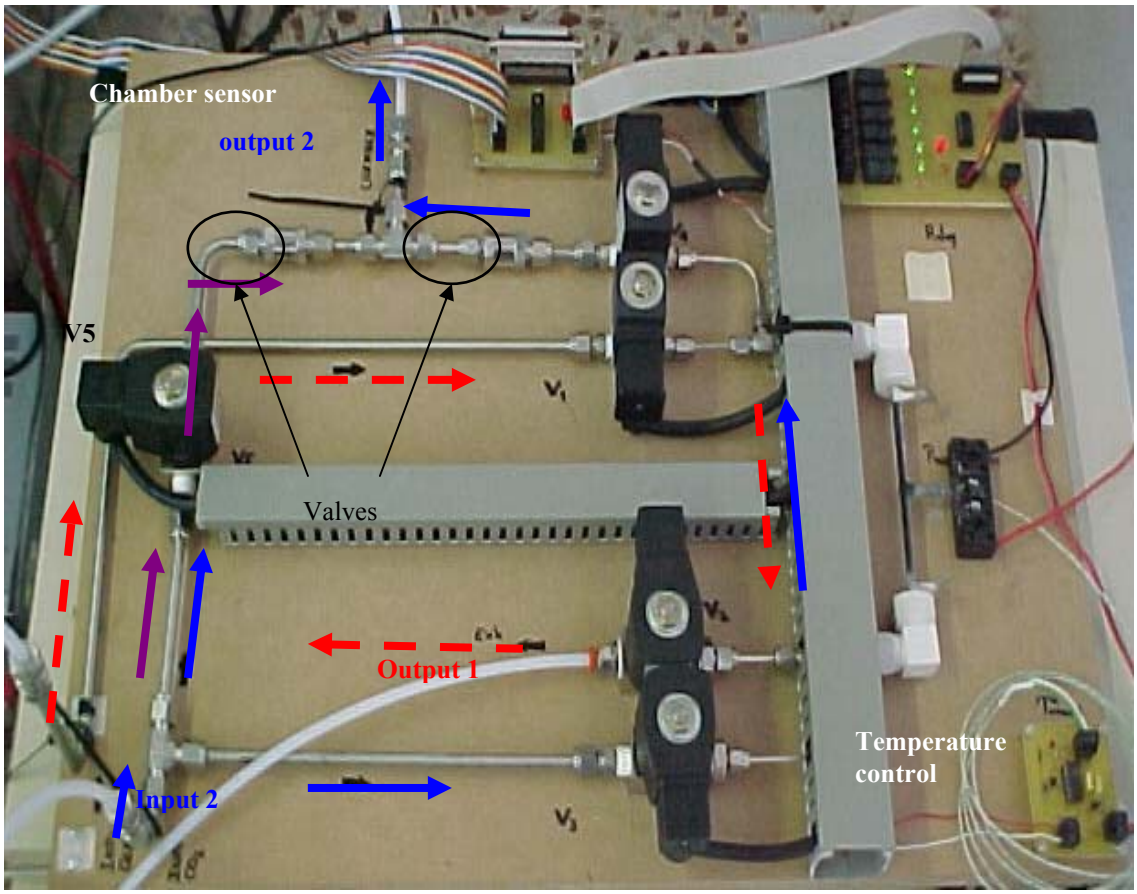

Figure 7: The final system configuration with the different subsystems

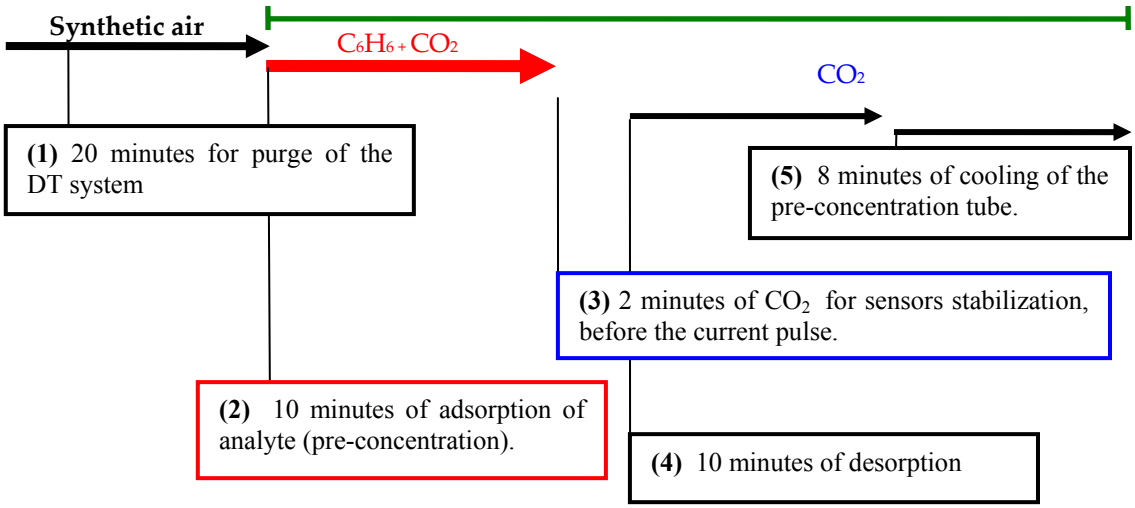

Figure 8: Chronogram of the measurements made with the prototype

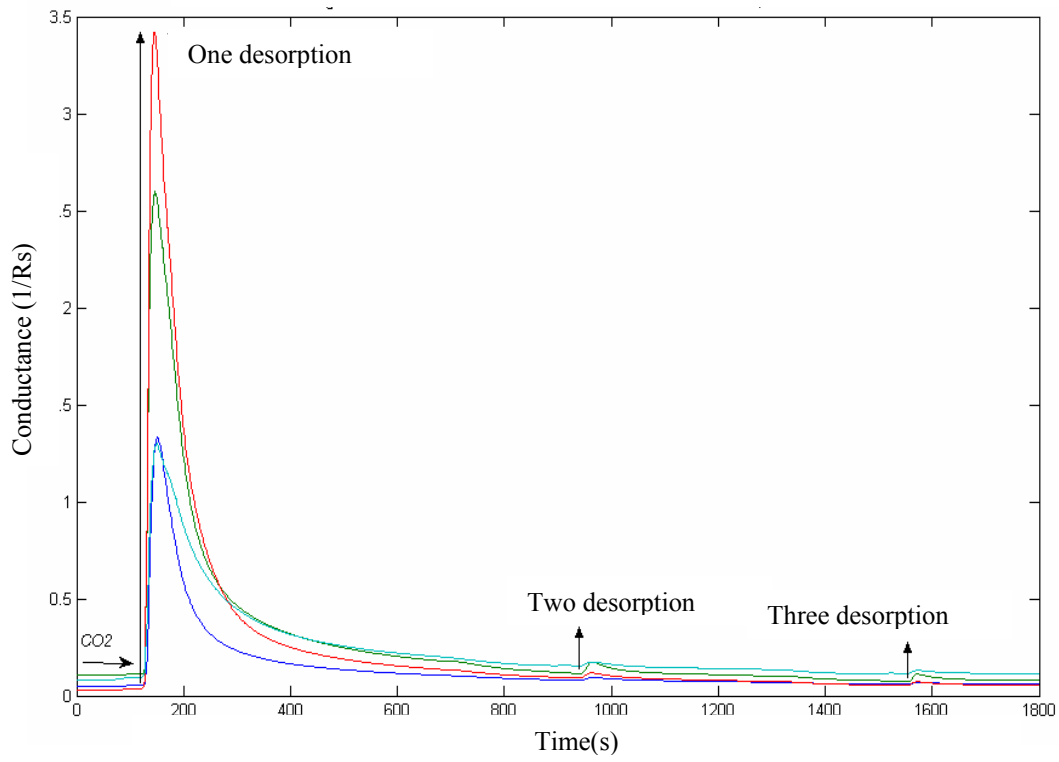

Figure 9: Sensor array response to three consecutive desorptions

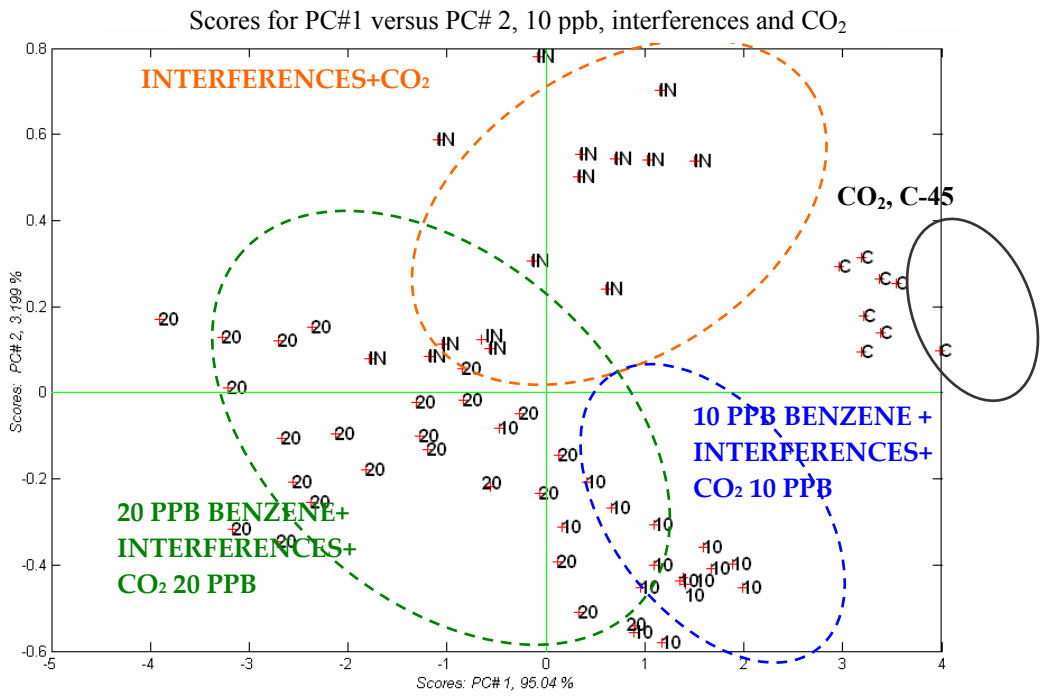

Figure 10: PCA graph with different types of cluster (10 ppb, 20 ppb, interferences and CO_2)

Pollutant	Maximum concentration allowed
Water	8 ppm
Total aldehydes	200 ppb
Ammonia	2 ppm
Benzene	**20 ppb**
Nitrogen dioxide	500 ppb
Sulfide dioxide	2 ppm
Heavy hydrocarbons	1 ppm
Volatile hydrocarbons	20 ppm
Methane	30 ppm
Carbon monoxide	2 ppm
Nitrogen	40 ppm
Nitric oxide	2.5 ppm
Oxygen	9 ppm
hydrogen Sulphide	500 ppb

Tabla 1: Tipical contaminants with their maximum concentrations allowed in 99.95 % purity CO_2

Amount	Type	Application
	Taguchi (Series -8)	
1	TGS-800	Air quality, smoke, benzene
2	TGS-821	hydrogen
1	TGS-880	Nourishing product scents
1	TGS-813	Combustible gas
1	TGS-842	Methane, natural gas
2	TGS-822	Organic dissolvents
2	TGS-823	Organic dissolvents (benzene)
2	TGS-826	Ammoniac
	FIS (Series -SP)	
2	SP-MW0	General intention. Kitchen control.
2	SP-11-00	General Purpose. Inflammable steam
2	SP-53	Hydrocarbons
2	SP-AQ2-00	Air quality, VOC's
2	SP-AQ3-00	Combustible gas

Tabla 2: Metal oxide sensors

Sensor	Normalized Conductance (Gmax-Gi)/Gi
TGS 800	0.6011
TGS 822	0.7648
TGS 823	1.3995
SP 31	1.4926

Table 3: Sensors chosen after determining the best sensitivities (defined as the normalized conductance increment).

# test	Current (A)	100 °C (seconds)	150 °C (seconds)	200 °C (seconds)	250 °C (seconds)
1	4,40	1,5	2,55	5,5	6,5
2	4,43	1,5	2,5	5,2	6,3
3	4,45	1,2	2,3	5	6
4	4,45	1,2	2,2	5	6
5	4,50	1	2	4	5
6	4,55	1	2	4	5

Tabla 4: Temperatures and transient times achieved by thermal desorption unit

Adsorbent	Mesh	Surface Area (m^2/g)	Density (g/mL)	Aplication
Carbopack B	60/80	100	0.36	C_5-C_{12}

Tabla 5: Characteristics of the material

Compound	Mixture
20 ppb benzene (C_6H_6) + 5 ppm Methane (CH_4) + 2 ppm CH_3OH (Methanol + CO_2	**(A)**
20 ppb benzene + 25 ppm Methane (CH_4) + 10 ppm CO + CO_2	**(B)**
CO_2 C-45	**(C)**
20 ppb benzene (C_6H_6) + CO_2	**(D)**
0.1 ppm SO_2 + CO_2	**(E)**
(E) + 20 ppb benzene + CO_2	**(F)**
25 ppm Methane (CH_4) + 10 ppm CO + CO_2	**(G)**
(G) + 20 ppb de benzene + CO_2	**(H)**
5 ppm of Methane + 2 ppm methanol + CO_2	**(I)**
(I) + 20 ppb de benzene + CO_2	**(J)**
4 ppm Methanol + CO_2	**(K)**
(K) + 20 ppb de benzene + CO_2	**(L)**
1.5 ppm (Argon + O_2) + CO_2	**(M)**
(M) + 20 ppb benzene + CO_2	**(N)**

Table 6: Different mixtures measured with 20 ppb of benzene

Compound	Mixture
CO_2 C-45	**(1)**
10 ppb benzene + 4 ppm de methanol + CO_2	**(2)**
10 ppb benzene + 5 ppm methane (CH4) y 2 ppm methanol + CO_2	**(3)**
10 ppb benzene + 25 ppm methane (CH_4) + 10 ppm CO + CO_2	**(4)**
10 ppb benzene (C_6H_6) + 0.1 ppm de SO_2 + CO_2	**(5)**
10 ppb benzene (C_6H_6) + CO_2	**(6)**
10 ppb + 1.5 ppm de O_2 + Argon + CO_2	**(7)**

Table 7: Different mixtures measured with 10 ppb of benzene

# measurement	Compound	Codification
24	20 ppb of benzene + interferences + CO_2	20
18	10 ppb of benzene + interferences + CO_2	10
15	Interferences + CO_2	IN
8	CO_2	C

Table 8: Different mixtures measured and their codification to classification

Normalization method	Success rate with the fuzzy ARTMAP
Auto-escalado	89 %
Centrado	84 %
Normalización por matriz	89 %
Normalización por sensor	87 %

Table 9: Classification with 4 categories (10 ppp, 20 ppb, interferences and CO_2 pure)

Normalization method	Success rate with the fuzzy ARTMAP
Auto-escalado	97 %
Centrado	92 %
Normalización por matriz	95 %
Normalización por sensor	94 %

Table 10: Classification with 3 categories (10 ppb with 20 ppb, interferences and CO_2 pure)

"Fast detection of rancidity in potato crisps using e-noses based on Mass Spectrometry or gas sensors", Sensors and Actuators B, Volume 106, Issue 1, 29, Pág: 67-75 (2005).

Available online at www.sciencedirect.com
SCIENCE DIRECT®
Sensors and Actuators B 106 (2005) 67–75
SENSORS AND ACTUATORS B CHEMICAL
www.elsevier.com/locate/snb

Fast detection of rancidity in potato crisps using e-noses based on mass spectrometry or gas sensors

M. Vinaixa [a], A. Vergara [a], C. Duran [a], E. Llobet [a,*], C. Badia [b], J. Brezmes [a], X. Vilanova [a], X. Correig [a]

[a] *Department Electronic Engineering, Universitat Rovira i Virgili, Avda. Països Catalans, 26, Campus Sescelades, 43007 Tarragona, Spain*
[b] *Frit Ravich, S.L., Pol. Ind. Puigtió s/n, 17412, Maçanet de la Selva, Girona, Spain*

Available online 2 July 2004

Abstract

Well-established methods to assess rancidity in potato crisps such as the Rancimat or the acid degree value are time-consuming and labour-intensive. Here, we report on alternative methods, based on e-nose technology, to assess rancidity directly from potato crisps without any previous oil extraction step. This simplifies sample preparation, avoids the use of solvents or high temperatures and significantly speeds up the measurement process (from several hours down to 25 min). Two different e-noses were implemented. One was based on SPME coupled to fingerprint MS and the other one was based on dynamic headspace sampling and an array of metal oxide gas sensors. The two e-noses were used to classify crisps according to four stages of oxidative rancidity. While the MS e-nose reached a 100% success rate in this classification, the success rate of the GS e-nose was 68%. These results show that e-nose technology can be a useful tool for the crisp industry.

We show that it is possible to reliably assess rancidity in potato crisps by either a mass spectrometry or a gas sensor-based electronic nose. The two approaches are presented and their performance compared in the framework of this application.

Keywords: Metal oxide gas sensors; Mass spectrometry-based e-nose; Crisp rancidity

1. Introduction

Potato crisps are considered one of the most popular snack products in the world. Usually, they are made by deep-frying fresh potato slices in a vegetable oil bath. The reaction of lipid components with oxygen in the presence of light and heat is a major source of off-odours/flavours in food and, particularly, in potato crisps. During the deep-frying process, vegetable oil is under temperature stress and this can induce onset of rancidity as a consequence of oxidative reactions of lipids present in the oil. From the standpoint of food oxidation, the important lipids are the ones containing unsaturated fatty acids, particularly oleic acid (C18:1), linoleic acid (C18:2) and linoleic acid (C18:3) [1]. Potato crisps are fried in oils that contain a high amount of all of these. Unsaturations are reactive centres liable to be affected by oxidation. So, the greater the number of double bonds, the higher the probability that the fatty acid will react with oxygen to generate undesirable odours and flavours in the product. The oxidation of lipids results in the formation of primary and secondary decomposition products, including hydroperoxides, carbonyls, alcohols, esters, carboxylic acids and hydrocarbons [2], which generally have unpleasant odour and may conduce to rancidity. Various factors can influence the occurrence of rancidity in crisps, such as storage conditions, presence of antioxidants, oil type, time of deep-frying, heat, presence of pro-oxidant metals, oxygen and moisture among other factors.

Two very important aspects for potato crisps producers are the detection of rancidity and its associated off-odours/flavours and the estimation of shelf-life. There are basically two reasons why it is important to monitor to what extent oil has undergone oxidation:

- Previous knowledge, i.e. an estimate, on the useful life of frying oil contributes to reduce the cost of the deep-frying process. There is an obvious economic advantage when crisp producers can appropriately determine the useful life of frying oils. Premature discarding of oils results in economic loss and, on the other hand, overuse of frying oil greatly affects the quality of fried products and causes undesirable nutritional effects [3].

* Corresponding author. Tel.: +34 977 558502; fax: +34 977 559605.
E-mail address: ellobet@etse.urv.es (E. Llobet).

0925-4005/$ – see front matter © 2004 Elsevier B.V. All rights reserved.
doi:10.1016/j.snb.2004.05.038

- The second reason is an ever increasing consumer about quality and safety of food products. According to Marsili [4], the food industry needs the development of equipment and techniques to trace the quality of raw materials and finished products, not only in the production plant, but also during storage and vending. Monitoring of off-odours/flavours during the different processing steps should be conducted to ensure that the processes are being operated correctly. Finished products should be monitored too, ensuring that no off-flavours have developed. All these improvements would greatly contribute to food quality and consumer satisfaction.

Nowadays, there are some 360 procedures to verify the quality of oil either during the process of frying or in finished products [1,5]. However, there is not a reliable, easy-to-use and fast method to determine rancidity in potato crisps. The most well-established methods for the evaluation of rancidity are based on sensory evaluation or chemical analysis. Some of these methods are revised below:

- Sensory analysis: Samples are evaluated by a panel of experts. This is a slow and expensive method. It requires the panel to be integrated by highly trained personnel and, however, results can be somewhat subjective.
- Peroxide value (PV): This method determines all the substances, in terms of milliequivalents of peroxide per gram of sample, which oxidise potassium iodine under the conditions of the test. These substances are generally assumed to be peroxides or other similar products of fat oxidation. The higher the PV, the more oxidised the fat is and the higher the likelihood of off-odours/flavours.
- Acid degree value (ADV): This is a titration method. It obtains the amount of potassium hydroxide required to neutralise the free fatty acids hydrolysed with 95% ethanol. The higher the ADV, the higher the level of free fatty acids present in the oil. Free fatty acids indicate undesirable hydrolysis, which results in flavour deterioration. Che Man et al. [3] showed that ADV was an important indicator of frying oil quality, and highly correlated with the shelf-life of potato chips.
- Iodine value (IV): Indicates the number of double bonds or degree of unsaturation in lipids. It can be used as an estimate of the oxidation stability of a lipid.
- HPLC analysis: Determination of the fatty acid composition of oil. This method provides fatty acid profiles and is more informative than IV.
- IR an UV band absorption of some oxidation by-products like hexanal, pentanal and pentane.
- Methods based on the measurement of some physical properties of oil, such as melting point, solid fat index and refractive index.
- Rancimat test: Measures the susceptibility of oil to oxidation. An oil sample is kept at 120 °C in a vessel where air flows to extract volatiles from the headspace. These volatiles are then collected in water. The conductivity of water is monitored and results expressed as Rancimat hours indicate the time at which oxidative rancidity occurs. Rancidity triggers a sharp increase in water conductivity. Since this test is very informative about the resilience to rancidity of oils, it has become a reference in the crisp industry.

All the methods cited above can be used to assess rancidity in potato crisps, provided that a process to extract oil from the crisps is performed. Oil extraction is a very time-consuming, complex and labour-intensive step for routine quality control applications. Furthermore, the solvents or the methods used can induce oxidation and distort final results. Since the crisp industry demands a large number of samples to be analysed and high sample throughput, there is a need for faster and simpler methods to assess crisp rancidity and off-odours/flavours. In this context, the use of e-nose technologies would be of help.

In the last decade, the use of e-nose technology in many food-related applications has been studied. Electronic noses are multisensor instruments that use a suitable pattern recognition engine to classify complex odour patterns. According to previous works, electronic noses based on metal oxide gas sensors are suitable for the discrimination of different stages of lipid oxidation in oils [6–8]. In the last few years, mass spectrometry-based e-noses (MS e-noses) are becoming an increasingly used alternative (or complement) to gas sensor-based e-noses in food quality applications [4,9]. The use of pre-concentration and extraction techniques such as solid-phase micro-extraction (SPME) have improved the sensitivity and reproducibility of MS e-noses [4,10].

In this work, we report, for the first time, on the design and use of two e-noses to assess rancidity directly from potato crisps, without any previous oil extraction step. This greatly simplifies sample preparation, avoids unwanted artefacts derived from oil extraction and speeds up the measurement process. The two e-noses are based on SPME–MS and an array of semiconductor gas sensors (GS e-nose), respectively. In the next section, details on the e-nose architectures sample preparation and measurements run are given. In Section 3, the results are shown and the usefulness of the methods implemented for the application considered is discussed.

2. Experimental

2.1. Experiment 1

2.1.1. Crisp samples

Four boxes (labelled *A–D*) with 200 g packs (12 packs per category) of potato crisps were prepared by Frit Ravich, S.L. These crisps belonged to the same frying batch of 50% palm and 50% sunflower oil, but they underwent different rancidity accelerating treatments:

- Crisps in box *A* were stored during 28 days in a dry and dark conservation chamber, where their temperature was kept around 20 °C.

- Crisps *B–D* were kept during 14, 21 and 28 days, respectively, in a rancidity accelerating chamber. The chamber was kept at high temperature (around 40 °C) and UV light was used to promote oxidation. As soon as the samples within a given category finished their ageing treatment, they were removed from the rancidity chamber and stored in the conservation chamber to maintain unchanged the rancidity stage reached.

2.1.2. Measurement procedures

The content of each potato pack was split to perform consistent measurements with an MS e-nose and a GS e-nose.

2.1.2.1. Metal oxide sensors-based electronic nose. The electronic nose system was designed to measure volatiles directly from the packs of the crisps. The system consisted of a sensor chamber where seven TGS-type sensors and five FIS sensors were housed, several electrovalves, tubing and a pump (see Fig. 1a). A similar set-up is described elsewhere [11]. The measurement procedure consisted of two steps. In the first step, (measurement phase) the electrovalves were set to form a closed loop between the sensor chamber and the pack containing the crisps under analysis. The air flow (150 ml/min) was re-circulated, which caused a dynamic sampling of the crisps' headspace. During this phase, which lasted 10 min, the resistance of the sensors was acquired and stored for later processing. Finally, in the second step (cleaning phase), the crisp pack was removed and the system was cleaned with dry air during 20 min before a new measurement could start.

After a pack of crisps had been measured by the GS e-nose, 4 ± 0.2 g of the crisps were crushed and put into a 20 ml vial that was immediately capped and sealed with a Teflon septum. A subsequent analysis with the MS e-nose system was run.

2.1.2.2. Mass spectrometry-based electronic nose. A Shimadzu QP 5000 gas chromatograph–mass spectrometer was used to implement an MS e-nose. The separation column was replaced by a 5 m deactivated fused silica column to co-elute all volatile components achieving one single peak for all the components in the headspace of crisps. The column

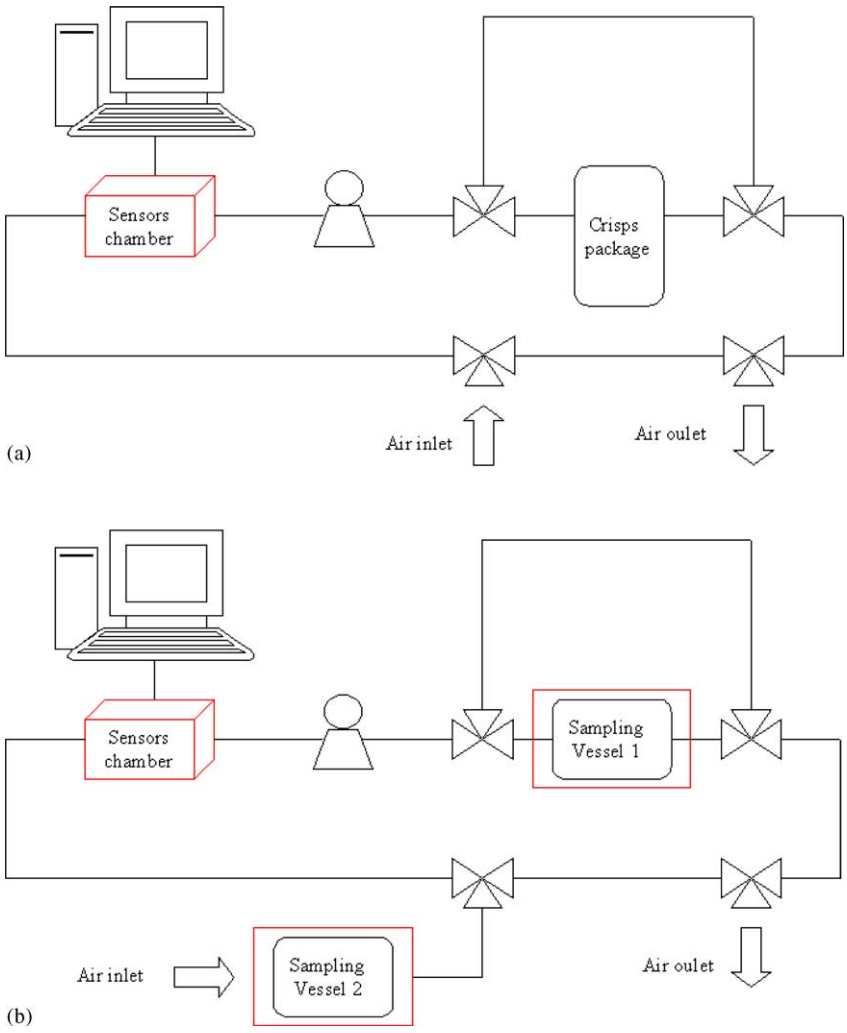

Fig. 1. Block diagram of the gas sensor-based e-nose used in experiment 1 (a) and experiment 2 (b).

was kept isothermal at 250 °C and the helium flow was set to 1.4 ml/min. This implies that the components in the headspace of crisps were directly analysed without chromatographic separation. For a given measurement, the resulting mass spectrum gives a fingerprint that is characteristic of the volatiles present in the headspace of the sample.

The vials that contained the samples to be measured were placed inside a thermostatic bath (50 °C) to promote the presence of volatiles in the headspace. SPME was performed by introducing a 75-μm Carboxen/PDMS fibre into the vial and exposing it to the headspace of crisps for 20 min. Thermal desorption of the volatiles trapped on the fibre was conducted for 3 min in the chromatograph injection port at 300 °C. It was equipped with a 0.75-mm i.d. liner to optimise SPME desorption and sample delivery onto the column The split valve was closed during desorption. The quadrupole mass spectrometer acquired in scan mode, and the mass range used was *m*/*z* 35 to *m*/*z* 390 at 0.5 scan/s. To ensure the complete cleaning of the fibre, it was left five additional minutes in the injector port.

2.1.2.3. Rancimat, ADV and chromatographic profiles. Rancimat and ADV tests were performed at the quality laboratory of Frit Ravich, S.L. The chromatographic profiles were obtained at the Gas Sensor Lab of the University Rovira i Virgili, using a Shimadzu QP 5000 GC/MS. After sample preparation (as described above), the SPME fibre was introduced into the GC injection port and thermally desorbed for 5 min at 250 °C onto an Equity-5 poly (5%diphenyl/95% dimethylsiloxane) (30 m × 0.25 mm × 0.25 μm) capillary column, purchased from Supelco Inc. The injector port was also equipped with a 0.75-mm i.d. liner. The GC oven was held at 45 °C during 1.5 min. Then, its temperature was raised up to 250 °C at 6 °C/min rate. Helium at 1.2 ml/min was used as carrier gas. Mass detector was operating in the electron impact ionisation mode (70 eV) with a scan range of 35 to 290 amu. The ion source temperature was kept at 250 °C.

2.2. Experiment 2

A new experiment was performed with an improved version of the gas sensor-based electronic nose. The main differences with the previous system were the use of a 12-element TGS-type sensor array (the seven TGS sensors already used in the first experiment + five TGS sensors added) and a new sample delivery method.

2.2.1. Crisp samples

Four boxes (labelled *A–D*) with 200 g packs of crisps (12 packs per category) were prepared by Frit Ravich S.L. in a similar way to the crisps used in experiment 1.

- Crisps in box *A* were stored during 18 days in the same conservation chamber used in experiment 1.
- Crisps *B–D* were kept during 6, 12 and 18 days, respectively, in the rancidity accelerating chamber used in experiment 1.

2.2.2. Improved gas sensor-based e-nose

The sample delivery system consisted of two temperature-controlled stainless-steel vessels (see Fig. 1b): a sampling vessel and a reference vessel. These chambers were identical and kept heated at 70 °C. To run a measurement, crisp samples (60 ± 1 g) were placed into an aluminium tray and inserted into the sampling vessel. An identical (but empty) aluminium tray was also placed inside the reference vessel. New aluminium trays were used at each new measurement to avoid cross-contamination between samples. The measurement procedure was as follows:

In the first step (concentration phase), the crisps were heated at 70 °C for 30 min inside the sampling vessel, which was kept closed by the electrovalves. This allowed the volatiles from the crisps to concentrate in the headspace. During this phase, clean air flowed at 150 ml/min through the sensor chamber via the reference vessel.

In the second step (measurement phase), the electrovalves were set to form a closed loop between the sensor chamber and the sampling vessel. The air flow (150 ml/min) was re-circulated, which caused a dynamic sampling of the crisps' headspace. During this phase, which lasted 10 min, the resistance of the sensors was acquired and stored for later processing. The use of identical sampling and reference vessels is essential to ensure that sensor responses are solely due to the volatiles in the headspace of the crisps.

Finally, in the third step (cleaning phase) the crisps were removed from the sampling vessel and the system was cleaned with dry air during 20 min, before the concentration phase of a new measurement could start.

3. Results and discussion

3.1. Experiment 1

3.1.1. Rancimat, ADV and chromatographic profiles

Fig. 2(a) shows the Rancimat and ADV results for crisp samples *A–D* in experiment 1. The monotonous decrease in Rancimat time combined with an increase in the ADV for samples *A–D* shows that these categories correspond to crisps with increasing oxidative rancidity. Furthermore, the clear differences in Rancimat time between categories suggest that crisps in different categories are in significantly different rancidity stages. While there is an important difference in Rancimat time between samples *A* and *B*, they share an almost identical ADV. This suggests that ADV may not be suitable to assess the early stages of rancidity in crisps.

Chromatographic profiles of the headspace of crisps belonging to class *A* (fresh) and class *D* (rancid) were

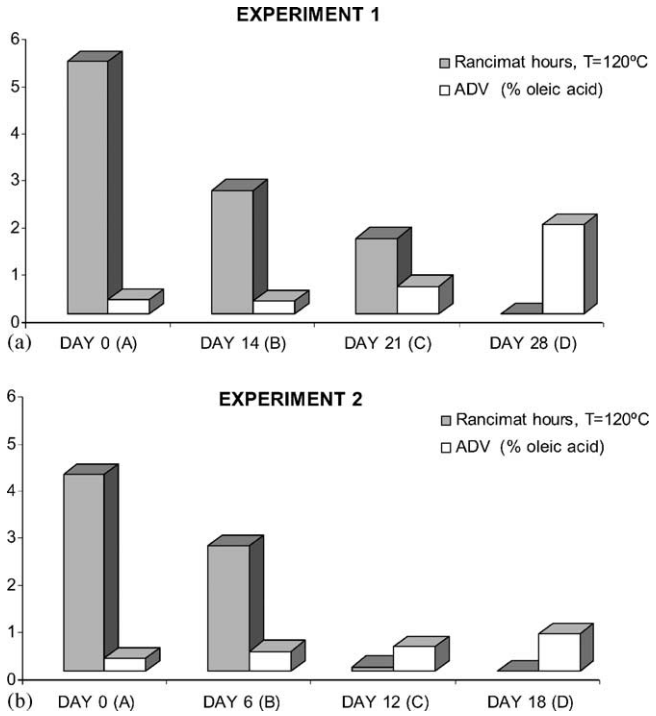

Fig. 2. Results of the Rancimat and ADV tests for potato crisps in eperiment 1 (a) and experiment 2 (b).

measured. These profiles are shown in Fig. 3. Different volatile molecules appear or substantially increase their signal intensity as rancidity develops. These include acetone (peak no. 1), acetic acid (2), pentanal (3), hexanal (5), heptanal (6), hexanoic acid (9), 3-octen-2-one (10), 2-octenal (11), 2,3-octanedione (12), 2,4-decadienal (14) and undecane (15). Some of these components, such as acetic acid, pentanal, hexanal, heptanal and hexanoic acid, have been reported to be present in the chromatographic profiles of rancid chips [12]. 2,4-decadienal [14], which is present in a similar intensity in fresh and rancid crisps, has been identified by GC-olfactometry [13,14] as a predominant note in deep-fried potato crisps.

3.1.2. Mass spectrometry-based e-nose

Nine replicate measurements per sample category were performed. For each measurement, a response spectrum was obtained by averaging mass spectra along the detected peak. The variables selected were from *m*/*z* 35 to *m*/*z* 120. The components identified as indicators of rancidity in the cromatographic profiles have base peaks that lie in the range selected. Therefore, the data matrix, ***R***, consisted of 86 columns (variables) and 36 rows (measurements). A linear discriminant analysis (LDA) was performed on ***R***. This is a supervised method (e.g. the classes to be discriminated are known before this analysis is performed). Geometrically, the rows of the response matrix, ***R***, can be considered as points in a multidimensional space. Discriminating axes are determined in this space in such a way that optimal separation of the predefined classes is attained. Like PCA, LDA finds new orthogonal axes (factors) as a linear combination of the input variables. Unlike PCA, however, LDA computes the factors as to minimise the variance within each class and maximise the variance between classes. The first factor will be the most powerful differentiating dimension, but later factors may also represent additional significant dimensions of differentiation.

The data matrix was mean-centred before the LDA was performed. If this scaling of the data is not performed, there is a risk of LDA ignoring mass intensities with low mean (but important for discriminating the four rancidity classes) in front of mass intensities with high mean. The two first factors accounted for more than 99% of the variance in the data. LDA results are shown in Fig. 4. Replicate samples of a given category cluster together with low dispersion, which shows the good repeatability of the MS e-nose. Fig. 4 shows that crisp samples with increasing rancidity appear ordered from left to right along the first factor. While samples from categories *A* (fresher) and *D* (more rancid) appear in clusters well apart, the clusters of categories *B* and *C* are very near. These results are in very good agreement with the Rancimat tests (see Fig. 1a). For example, while there is a moderate change in the Rancimat time between samples in categories

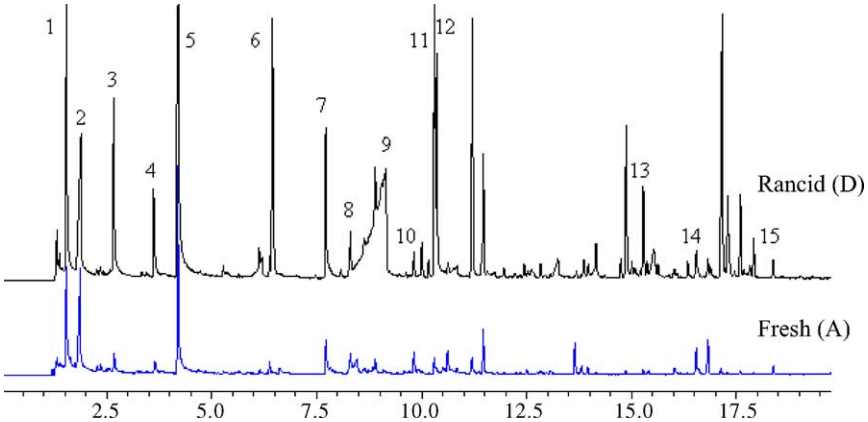

Fig. 3. Chromatographic profiles identified by GC/MS (1) acetone, (2) acetic acid, (3) pentanal, (4) pentanol, (5) hexanal, (6) heptanal, (7) 2-heptenal, (8) 1-octen-3-ol, (9) hexanoic acid, (10) 3-octen-2-one, (11) 2-octenal, (12) 2,3-octanedione, (13) 2-decenal, (14) 2,4-decadienal, (15) undecane.

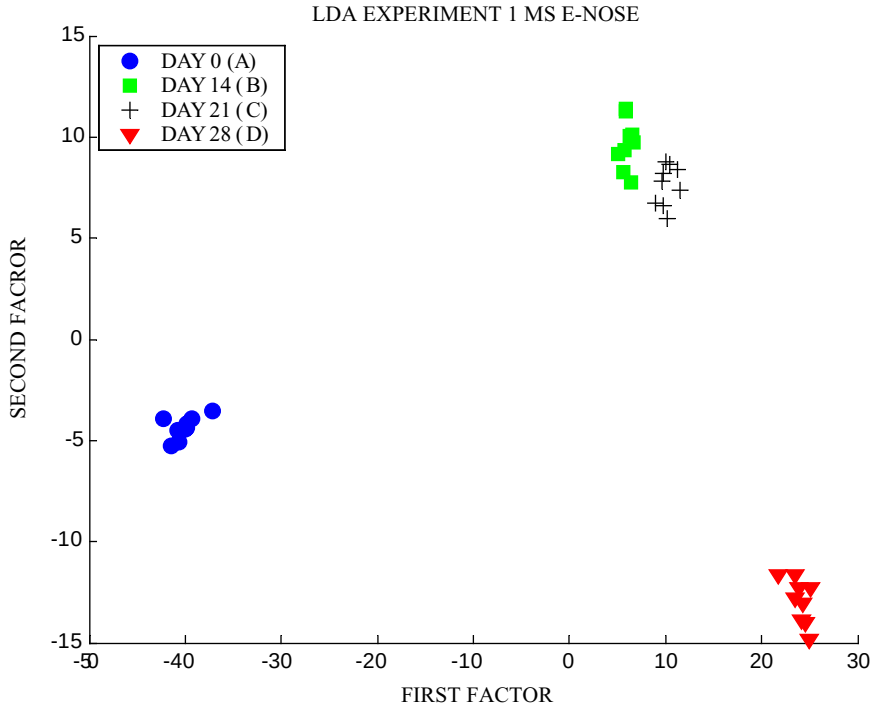

Fig. 4. Results of a linear discriminant analysis for the measurements gathered with the mass spectrometry-based e-nose in experiment 1.

B and C, there is a dramatic change in this parameter between samples in categories *A* and *B* and also between samples in *C* and *D*. Therefore, MS e-nose results are in excellent agreement with Rancimat results.

A fuzzy ARTMAP neural network was used to classify the samples within the four categories of rancidity (*A–D*). Because of the limited number of measurements available (36), the network was tested using the leave-one-out cross-validation method. Given n measurements, the network was trained n times using $n - 1$ training vectors. The vector left out during the training phase (i.e. unseen by the network) was then used for testing. Performance was estimated as the averaged performance over the n tests. For each iteration of the cross-validation process, a different row from the data was left out. The remaining 35 rows conformed the restricted data matrix. A pre-processing step was performed on the restricted data matrix, which consisted of computing a 4-class LDA and retaining the two first factors. The scores of the 35 measurements conformed the new data matrix. Therefore, this new matrix had 35 rows and 2 columns. The matrix was then normalised because the fuzzy ARTMAP network needs that its input data lie in the range [0, 1]. Once the data matrix had been pre-processed, it was used to train the neural network model. After the training phase, the network was validated using the vector that had been left out (i.e. validation vector). The procedure was as follows:

Because a LDA had been used as pre-processing, then the scores of the validation vector were calculated by projecting its components onto the space of factors. In the second step, the validation vector was normalised. Finally, the validation vector was input into the neural network model, which produced a classification result. The fact that the validation vector had been left out before any pre-processing of the data ensured that this vector was completely ‘new’ for the neural network.

The number of inputs to the network was set to 2 (the scores on the two first factors). The number of outputs was set to 4 because a 1-of-4 code was used for the different classes (*A*: 0001, *B*: 0010, *C*: 0100 and *D*: 1000). For example, the activation of the first output neurone (i.e. output pattern 0001), implies that an input vector is recognised as belonging to class *A* (fresh crisps). This approach aimed at identifying rancidity in a semi-quantitative way. The baseline vigilance parameter was set to 0. This is the recommended value for the vigilance since it allows for very coarse categories and the match tracking system will only refine these categories if necessary. The re-code rate was set to 0.5. This value allows the established categories to be modified if there is a persistent attempt to do so (slow recode). The value of the choice parameter was set to 0.1. The Fuzzy ARTMAP network could learn the training set in just one iteration. The number of committed nodes, which play a similar role as hidden neurones in multilayer perceptron networks, ranged between 4 and 6 after the network had been trained. Under these conditions, the success rate reached in rancidity classification was 100%. This shows that the SPME–MS e-nose was able to assess crisp rancidity from the volatiles present in the headspace of the crisps.

3.1.3. Gas sensor-based e-nose

The responses of the 12 metal oxide gas sensors to the different crisp samples were obtained. The feature extracted from each sensor response was the conductance change, defined as $\Delta G = G_{max} - G_o$, where G_{max} is the maximum value of the sensor electrical conductance in the presence of the volatiles from the headspace of the crisps, and G_o is the sensor conductance in the presence of air (i.e. the baseline conductance). The responses of the FIS sensors were very weak compared with the responses of the TGS sensors. Therefore, only the responses of the seven TGS sensors were used for further analysis. A LDA was performed on the mean-centred response matrix. The two first discriminant factors accounted for more than 99% of variance in the data. LDA results are shown in Fig. 5. While measurements that correspond to fresh crisps (class *A*) cluster together, the clusters of measurements corresponding to the remaining three classes appear clearly overlapped along the first and second discriminant factors. A fuzzy ARTMAP was used to classify the samples according to their rancidity stage. The same training and validation techniques employed with the MS e-nose were implemented. The neural network had seven inputs (seven TGS sensors) and four outputs. The number of committed nodes during the repeated training and validation processes varied between 8 and 12. Under these conditions, the success rate reached in rancidity classification was 56%. The samples misclassified belonged to categories *B–D*.

According to these results, the GS e-nose showed lower repeatability and discriminating power than the MS e-nose. However, an important difference between the two e-nose methods lies in sample preparation. While for the GS e-nose volatiles were sampled from the headspace of the crisps at room temperature, the MS e-nose made use of a SPME from the headspace of crisps heated at 50 °C. Therefore, the differences in classification success rate between the two e-noses could be due to significant differences in the headspaces sampled. This is why a new experiment was designed.

3.2. Experiment 2

3.2.1. Rancimat and ADV results

Fig. 2b shows the Rancimat and ADV results for crisp samples *A–D* in experiment 2. The oil used to deep-fry the crisps in experiment 2 had the same composition than the one used in the previous experiment. However its initial stage (class *A*) was, according to the Rancimat test, more evolved towards rancidity. The results of the Rancimat test showed that the classification of samples in four rancidity categories was going to be more challenging here, because samples in classes *C* and *D* had very similar Rancimat and ADV results.

3.2.2. Gas sensor-based e-nose

The GS e-nose with a re-designed sample delivery system was used. The responses of the 12 TGS-type metal oxide gas sensors to the different crisp samples in experiment 2 were obtained. The feature extracted from each sensor response was, once again, the conductance change. Since 12 replicate measurements per category were gathered, the response matrix had 48 rows and 12 columns. A LDA was performed on the mean-centred data matrix. The two first

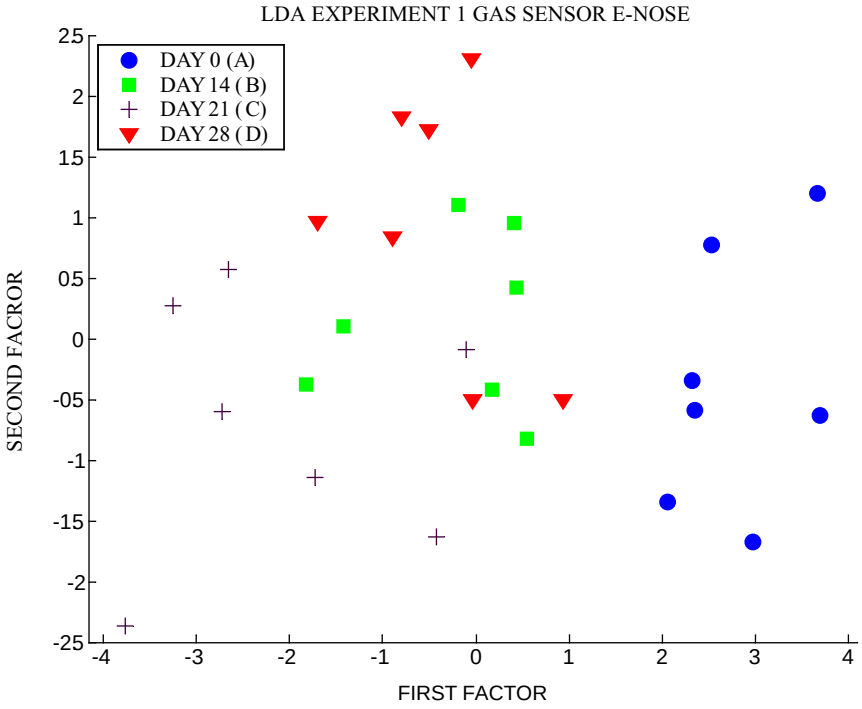

Fig. 5. Results of a linear discriminant analysis for the measurements gathered with the gas sensor-based e-nose in experiment 1.

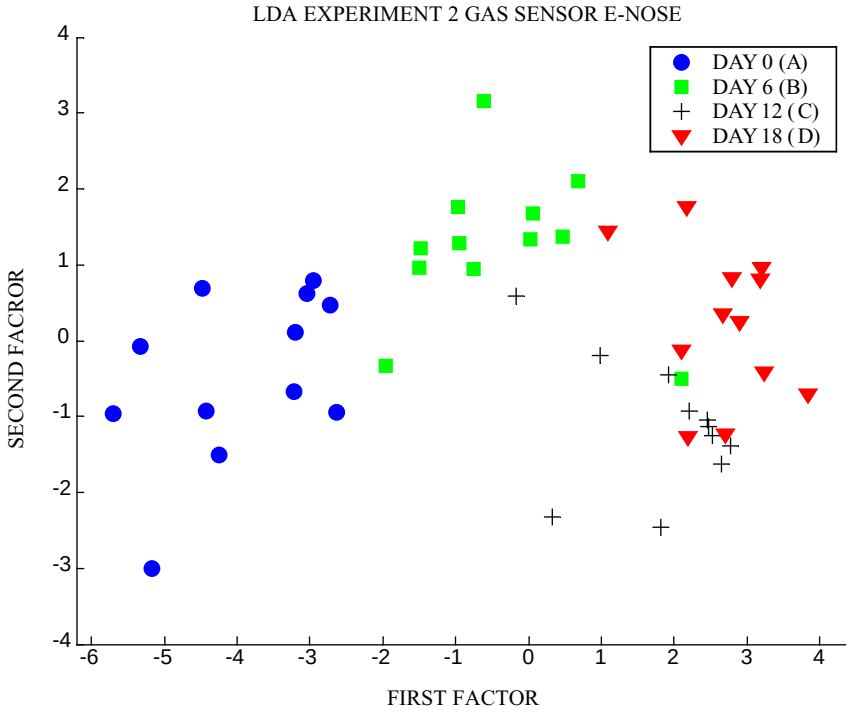

Fig. 6. Results of a linear discriminant analysis for the measurements gathered with the gas sensor-based e-nose in experiment 2.

factors accounted for more than 99% of variance in the data. LDA results are shown in Fig. 6. This figure shows that crisp samples with increasing rancidity appear ordered (with some overlapping) from left to right along the first factor. Overlapping occurs between samples in categories *C* and *D*, which is in good agreement with the very similar Rancimat times found for these categories. These results suggest that it is necessary to heat the crisps for a headspace that is representative of their rancidity stage to develop.

A fuzzy ARTMAP was, once again, used to classify the samples according to their rancidity stage. The same training and validation techniques employed in experiment 1 were implemented. The neural network had 12 inputs (12 TGS sensors) and 4 outputs. The number of committed nodes during the repeated training and validation processes varied between 7 and 10. Under these conditions, the success rate reached in rancidity classification was 68%. Considering that the classification problem envisaged in experiment 2 was more challenging, a 68% rate of successful classifications compares very favourably with the 56% success rate reached in experiment 1. Table 1 shows the confusion matrix for experiment 2. It can be seen that most confusions occur between consecutive rancidity categories (only two samples belonging to class *D* were misclassified as belonging to class *B*).

Table 1
Confusion matrix for the classification of crisps samples in four categories of rancidity (*A*–*D*) in experiment 2, using a fuzzy ARTMAP neural network

	Actual			
	A	*B*	*C*	*D*
Predicted as				
A	9	2	0	0
B	3	8	2	2
C	0	2	8	2
D	0	0	2	8

These promising results show that the GS e-nose with improved sample delivery system is able to perform a semi-quantitative classification of crisp rancidity.

4. Conclusions

In this work, we have reported on the design and use of two e-noses to assess rancidity directly from potato crisps, without any previous oil extraction step. This simplifies sample preparation, avoids the use of solvents to extract oil and speeds up the measurement process. The two e-noses were based on fingerprint mass spectrometry and an array of metal oxide gas sensors, respectively. While a single measurement using either the Rancimat or the ADV test takes typically some hours to complete, a measurement with the MS e-nose or the GS e-nose takes 25 and 40 min, respectively.

Sample conditioning plays a very important role. A mild heating of the crisps (up to 70 °C) is necessary for a headspace that is representative of their rancidity stage to develop. Under these conditions, the MS e-nose and the GS e-nose have been found sensitive enough and suitable for semi-quantitatively assessing rancidity in potato crisps. The results obtained by both e-nose instruments are in very good

agreement with the Rancimat test. Therefore, the assessment of crisp rancidity using e-nose technology could become a routine test in the quality laboratories of crisp producers.

Further work is in progress to analyse the shelf-life of potato crisps.

Acknowledgements

The authors gratefully acknowledge financial support from the Spanish Institute of Agro-Food Technology, INIA, under Project no. CAL01-052-C2.

References

[1] R. Marsili, Controlling the Quality of Fats and Oils, 1993. http://www.foodproductdesign.com.
[2] N. Shen, S. Duvick, P. White, L. Pollack, Oxidative stability and AromaScan analyses of corn oils with altered fatty acid content, J. Am. Oil Chem. Soc. 76 (12) (1999) 1425–1429.
[3] Y.B. Che Man, J.L. Liu, R.A. Rahman, B. Jamilah, Shelf-life of fried potato chips using palm olein, soybean oil and their blends, J. Food Lipids 6 (1999) 287–298.
[4] R. Marsili, Flavor, Fragance and Odor Analysis, Marcel Dekker, Inc., New York, 2002.
[5] AOCS, Official Methods and Recommended Practices of the American Oil Chemists' Society, fifth ed., 1998.
[6] M. Adechy, V.P. Shiers, J.B. Rossell, Study of rancidity and resistance to oxidation in edible oils and fats using electronic nose technology in comparison with conventional analytical techniques, Leatherhead Food R.A. Research Reports, no. 751, 1998.
[7] Y.M. Yang, K.Y. Han, B.S. Noh, Analysis of lipid oxidation of soybean oil using the portable electronic nose, Food Sci. Biotechnol. 9 (3) (2000) 146–150.
[8] M. Muhl, H.U. Demisch, F. Becker, C.D. Kohl, Electronic nose for detecting the deterioration of frying fat – comparative studies for a new quick test, Eur. J. Lipid Sci. Technol. 102 (2000) 581–585.
[9] R.T. Marsili, SPME–MS–MVA as an electronic nose for the study of off-flavors in milk, J. Agree. Food Chem. 47 (1999) 648–654.
[10] E. Schaller, S. Zenhäusern, T. Zesiger, J.O. Bosset, F. Escher, Use of preconcentration techniques applied to a MS-based "Electronic Nose", Analusis 28 (2000) 743–749.
[11] J. Brezmes, E. Llobet, X. Vilanova, J. Orts, G. Saiz, X. Correig, Correlation between electronic nose signals and fruit quality indicators on shelf-life measurements with pinklady apples, Sens. Actuators B 80 (2001) 41–50.
[12] R.E. Shirey, L.M.Sidisky, Analysis of Flavors and Off-Flavors in Foods and Beverages Using SPME, Supelco Application Note, http://www.infonew.sigma-aldrich.com/Graphics/Supelco/objects/8600/8564.pdf.
[13] R.K. Wagner, W. Grosch, Key odorants of french fries, J. Am. Oil Chem. Soc. 75 (10) (1998) 1385–1392.
[14] R.K. Wagner, W. Groshc, Evaluation of potent odorants of french fries, Food Sci. Technol. 30 (2) (1997) 164–169.